The Regional Meteorology of California Wildfire Emissions

Patrick Murphy

A thesis

submitted in partial fulfillment of the

requirements for the degree of

Master of Science

University of Washington

2022

Reading Committee:

Clifford F. Mass, Chair

Lynn A. McMurdie

Joel A. Thornton

Program Authorized to Offer Degree:

Atmospheric Science

University of Washington

Abstract

The Regional Meteorology of California Wildfire Emissions

Patrick Murphy

Chair of the Supervisory Committee:
Professor Clifford F. Mass
Atmospheric Science

Large, damaging, and costly wildfires associated with unusually strong, dry winds have occurred in California recently and through its history. This thesis examines the relationship between daily wildfire emissions and the observed regional meteorology for California's savanna and forest wildfires over the past 18 years. For each fuel type, the associated weather (daily maximum wind, daily vapor pressure deficient (VPD), and 30-day-prior VPD) is determined for all fire days, the first day of each fire, and the day of maximum emissions of each fire. Emissions for both savanna and forest wildfires are greatly modulated by regional meteorology, with the relationship between emissions and meteorology varying with the amount of emissions, fire location, and fuel type. Weak emissions are generally associated with climatological dryness and winds. For moderate emissions, increasing emissions are associated with higher VPD resulting from temperature increases and only a weak relationship with wind speed. High emissions, which constitute ~85% of the total emissions but only ~4% of the fire days, are associated with strong winds and large VPDs. Examining the meteorology during fires in subregions of California using spatial composites of surface variables, we find that weak-to-moderate

emissions are associated with modestly warmer than normal temperatures and light winds across the domain. In contrast, high emissions are associated with strong winds and substantial temperature anomalies, with colder than normal temperatures east of the Sierra Nevada and warmer than normal conditions over the coastal zone and the interior of California.

TABLE OF CONTENTS

LIST OF FIGURES

ACKNOWLEDGEMENTS

I would like to thank my advisor Cliff for giving me so much freedom as a graduate student to pursue what I have found interesting. I appreciate my committee members Joel—for showing me the GFED database and always answering my questions about the graduate process quickly—and Lynn—for teaching me so much mesoscale and synoptic meteorology. Additionally, I appreciate Professors Ernesto Alvarado and Brian Harvey of UW SEFS taking me under their wings and teaching me so much of the background and importance of fires and forest ecology; I have so much appreciation for wildfire now. I thank my undergraduate mentors, Professors Julie Lundquist and Jennifer Kay of CU Boulder as well as Dr. Paul Fleming at the National Renewable Energy Laboratory, for getting me to a point where I could join such a great graduate department at UW. Finally, thanks to UW Atmos staff, particularly Erica and Jennifer, for being so kind and quick to answer any and all questions I have had!

DEDICATION

This thesis is dedicated to my partner Erzsi, next to whom—literally, in our small apartment during COVID and lockdown— it was majorly worked on and written. I would also like to thank my parents for encouraging my curiosity from a young age and always fully supporting whatever it is I choose to do in my life. Finally, I give thanks to my favorite 15’x13’x50º haven of a climbing wall in south Seattle and the people it brings together.

Chapter 1
Introduction

1.1 History: wildfire in the Western United States

Wildfires are fires that occur in the combustible vegetation of the natural environment. Wildfires are complex, historically important, phenomena that are modulated by a range of factors from meteorological conditions to surface fuel conditions and ignitions (Keeley and Syphard 2018; Telford 2019; Mass and Ovens 2019; Brewer and Clements 2020). Since Earth's oxygen content and carbon based fuels have allowed them, wildfires have ignited for a multitude of reasons including lightning, falling rocks, and volcanoes (Agee 1993). There has never been a time since the earliest hominins walked the Earth in which Earth's climate did not support wildfire.

1.1.1 *Forests and fire*

Wildfires of varying severities have been an integral part of forest ecosystems for the last 400 million years (Franklin et al. 2002; Pyne 1996; Scott 2000; Scott et al. 2014). The three major regimes of forest fires during this time are high, mixed and low severity fires where severity is defined in terms of ecological consequence—for example by tree mortality, not intensity of fire as measured by temperature or flame length (Schoennagel et al. 2004; Sommers et al. 2011). These regimes have evolved with the fuels that support them and been reinforced through feedbacks that exist by coupling the fires and fuels (Steel et al. 2015).

In a typical high severity fire regime forest, fires occur infrequently due to a rarity of covarying ignitions and fire-enabling climatic conditions (Steel et al. 2015; Keeley and Syphard 2019). These characteristics enable mature older growth forests dominated eventually—both

throughout the canopy and in the understory—by vertically and horizontally diversified, shade-tolerant trees with relatively thin bark and a great amount of dead woody debris in the understory (Spies and Cline 1988; Franklin et al. 2002; Parker et al. 2002). If an ignition does occur, then given sufficient environmental conditions for fire to spread, the fires are likely to be stand replacing given the ladder fuels and lack of fire-resistant characteristics in individual species (Franklin et al. 2002; Schoennagel et al. 2004). These stand replacing fires clear both the canopy and understory and allow the regeneration and eventual coexistence of both fast-growing shade-intolerant "pioneer cohort" and slow-growing, late-successional, and shade-tolerant species (Franklin et al. 2002). In California, high severity regions are rare but may exist where conditions are climatologically cool, suppressing frequent fire and ignitions and allowing for decadent growing conditions. These may occur along the coasts or in high-elevation to subalpine Sierra Nevada forests (Van de Water and Safford 2011; Steel et al. 2015; Keeley and Syphard 2019). More common in California are mixed severity fire regimes—again usually cooler, wetter, or at higher elevation—but with somewhat alternating severities of fire in time in a given location (Stephens and Collins 2004; Steel et al. 2015). Spatially, certain high-elevation subregions may burn at longer intervals and with severe fire (Taylor and Solem 2001).

In a frequent, low severity fire regime forest, wildfires burn through the understory with lower intensity (Swetnam and Baisan 1996). This allows survival of mature trees with thick bark while clearing out young understory saplings, leaving few ladder fuels to enable crown—and thus stand replacing—fire. In these forests, the dominant tree species may approximate a monoculture (e.g., ponderosa pine[1]) of fast-growing, shade-intolerant trees with thick bark that are resistant to fire (Minore 1979; Hood et al. 2018). The lack of vertical and horizontal diversification aids an

[1]https://nfs.unl.edu/publications/downloads/Ponderosa%20Pine%20Forest%20Management%20and%20Silviculture%20-%20Final%20August%202015.pdf

open canopy and thus enhanced growing conditions (light, lack of competition) for regeneration of pioneer cohort descendants of the trees that drop their seeds following the fire ensuring the continued existence of such a low severity regime (Minore 1979; Hood et al. 2018; Parker et al. 2002; Parker et al. 2004). Non-forests, such as savanna (grasslands, shrublands, and chaparral) and woodlands (open stands of trees) often support low severity fire (Van de Water and Safford 2011; Steel et al. 2015; Keeley and Syphard 2019). Much of California is covered with fuels that historically allow low severity fire including the aforementioned non-forests and low elevation forests (Van de Water and Safford 2011; Steel et al. 2015).

Forest communities and fire share additional feedback mechanisms. Serotiny is the trait of closed gymnosperm cones opening following heat, allowing seeds to populate an area once a fire front has passed. This trait evidences more frequently in forest communities which were established by fire (Muir and Lotan 1985). This relationship suggests the existence of a positive feedback whereby plants that regenerate following fire have traits that make them more likely to succeed in regeneration and establishment following fire (Bond et al. 2004). Species in fire-prone regions may evolve increased flammability and post-fire regeneration traits such that their introduction into an ecosystem allows their species to preferentially catch fire, kill non-fire resistant and non-easily regenerated neighbors, and then regenerate themselves (Bond and Midgley 1995).

Because severe wildfires in modernity may be so human affecting (due to reasons addressed in Section 1.2 and beyond) and create for a few years (~5) what can be referred to as visual "hellscapes[2][3]" there are often popular misconceptions regarding the role of fire in natural

[2] https://www.forbes.com/sites/ericmack/2021/08/10/dixie-fire-hellscape-spawns-fire-devils-reaching-up-toward-air-traffic/?sh=199aacf668c7

[3] https://www.latimes.com/opinion/story/2020-09-09/wildfires-record-temperatures-hellscape-climate-change-greenland-rising-seas

ecosystems. Although severe wildfires by definition do have large ecological consequences in terms of plant mortality— by one definition, greater than 95% basal area burned and greater than 99% tree density mortality implying the few surviving trees are relatively large diameter and mature (Lydersen et al. 2016)—they serve important ecological functions. An ecological "sere" refers to the succession of plant communities which change in time, often bookended by severe disturbances which may restart a new sere.

The early seral forest (post stand replacing disturbance, for example: post severe fire), which may visually appear desolate compared to a mature forest, may often be the point highest biodiversity in a sere (Franklin and Spies 1991; Swanson et al. 2010; Swanson et al. 2014; Franklin et al. 2018). A forest which goes long enough without fire may evolve into an ecosystem type that fails to regenerate to its historical pattern, even following an eventual disturbance (Franklin et al. 2002). Additionally, although it may appear impossible to regenerate a complex ecosystem from a severely burned patch, around half to three quarters of a severely burned forest's area may still be within regeneration distance of surviving trees with the ability to reseed (Turner et al. 1994; Hood et al. 2018). Severely burned ecosystems described in the Turner et al. 1994 work recovered rapidly within 20 years post fire—or around 5% of an old growth sere's lifecycle assuming 400 year old trees typical of that subalpine ecosystem (Romme 1982; Romme et al. 2011).

In summary, plant ecosystems in the Western United States (U.S.) cannot—and should not—be thought of independently from fire.

1.1.2 *Wildfires and humans through the Holocene to modernity*

Historical fire did not just occur separately from humans; the fire that has occurred across the western United States (U.S.) throughout the Holocene was often human influenced (Pyne and Vale 2003). Recent work has shown that in the pre-industrial age across the southern Sierra Nevada,

native ignitions were more frequent than those of lightning in forested regions (Klimaszewski-Patterson et al. 2018). Native use of fire was sophisticated and was often part of a cultivation method through which rich soil would be developed (Agee 1993). Native Americans also set fires to facilitate hunting by flushing game out of wooded areas and creating clearings where they could more easily hunt in the future (Barrett and Arno 1999). Native fires were further used to wage war, communicate, open campsites and trails, and encourage the growth of grass as feed for horses (Barrett and Arno 1999). However, even across the western U.S. not all regions shared the same relationship between fire and humans. For chaparral-dominated landscapes, anthropogenic ignition of wildfire were minor compared to natural ignitions through early European settlement (Pyne and Vale 2003).

As Europeans and their descendants colonized the U.S., they dealt with fire and its effects. In 1804 in the Midwest, a region that now constitutes modern day Nebraska, Lewis and Clark's journals record that "the soil of these prairies appears rich but much parched with the frequent fires" (Clark 1804). Further along their journey in modern day Montana, Lewis and Clark moved their canoes underwater to protect them from "the fire which is frequently kindled in these plains by the natives" (Lewis 1805). In the late 19th century in the Pacific Northwest, Mark Twain and John Muir both remarked on thick smoke and burned trees (Agee 1993). Many of the fires of the late 1800's in the northwestern U.S. were human ignited (Morris 1934).

As settlers moved into the region and gained control of the forests, the fear of fire and anti-Native sentiment lead to general enforcement of fire suppression across the western U.S. (Agee 1993; Barrett and Arno 1999). In the early 20th century numerous efforts were developed to suppress forest fires (Agee 1993), with the greatest impetus provided by the wind-driven 1910 wildfire in Montana, the largest fire in U.S. history (Pyne 2001). The "Great Fire" of 1910 killed

nearly 100 people, destroyed multiple towns, and caused substantial financial damage to the timber industry (Pyne 2001). This fire and its contemporaries led directly to fire suppression practices which dominated the U.S. for the ensuing century (Pyne 2001). However, suppression was not practiced uniformly across the entire U.S., even after the 1910 fires. In certain regions of the Pacific Northwest, slash burns were encouraged or even mandated even as forest fire control reached a peak in the 1950's-1970's (Agee 1993).

In the past half century, policies and attitudes regarding forest fires have evolved. In the early 1970's policies began to shift to encourage controlled burns in forests following severe fires due to excessive undergrowth (Agee 1993). But environmentalist concerns, mainly dealing with air quality and ecological issues, resulted in constraints on the usage of fire for the ensuing decades (Agee 1993). Modern land management practice encourages a localized pragmatic results-based approach where different methods may be practiced in different areas (Schoennagel et al. 2004; Agee and Skinner 2005). However, practicing these methods on a large scale has proven challenging and costly, with recent funding cuts has increased risk of fire as well in recent years (Rossi and Kuusela 2019). Importantly, the overall decline in fires in the western U.S. during the past century has led to a deficit of fire, vastly increased fuel potential, and the increased potential for large catastrophic fires in historically frequent, low-severity fire regime regions (Schoennagel et al. 2004; Marlon et al. 2012).

Another important issue is that a growing population in rural areas during the past century has led to the growth of the area at the wildland-urban interface (WUI), greatly exacerbating the wildfire risk (Field and Jensen 2005; Hammer et al. 2007; Radeloff et al. 2018; Syphard et al. 2019). Anthropogenic land use changes, such as urban development into wildland areas, enhance fire ignitions, acreage, and structural loss (Syphard et al. 2019). Human fire ignition has increased

dramatically in many regions of the U.S. including California, lengthening the fire season, and is now more prevalent than natural ignition in most areas of the nation (Balch et al. 2017). Due to their proximity with urban areas, California's savanna regions are more frequently human ignited than forests, which are more often ignited by lightning. Fire exclusion practices dating back to the late 1800's have contributed to the increased frequency and intensity of California forest fires. Such exclusion has made California forests, which historically experienced frequent low-moderate severity fire, more susceptible to ignition and severe fire spread (Schoennagel et al. 2004; Collins et al. 2011; Marlon et al. 2012; Rossi and Kuusela 2019).

The increase in ignitions, lengthening of the fire season, mismanagement of forests, and increase in atmospheric temperatures and dryness from pre-industrial times act as compound disturbances (sensu Paine et al. 1998) that may have severe consequences—not just on mankind but on forests themselves. Regeneration failure is defined as the inability of an ecosystem to return to its preexisting state following a disturbance (Rammer et al. 2021). Such failure may be caused by repeated burns, compound or linked disturbance, or burns outside the natural severity regime (Simard et al. 2011; Halofsky et al. 2020). At present, regeneration failure has begun to occur in forests in Northern Canada which have already seen greater amounts of anthropogenic warming than the global mean and fire frequency beyond their historic fire regimes (Baltzer et al. 2021).

1.2 Motivation: wind driven fire in California

Major wildfires in the western United States have increased in acreage, societal impacts, and economic costs during the past several decades (e.g., Abatzoglou and Williams 2016; Dennison et al., 2014, Jones 2017; Parks and Abatzoglou 2020), with many of the largest and most impactful fires occurring in California (Littell et al. 2009; Nauslar et al. 2018; Addison and Oommen 2020; Brewer and Clements 2020). The role of dry conditions and strong, near-surface

winds has become evident, either at fire outset or during periods of rapid fire growth (Pagni 1993; Keeley et al. 2009; Moritz et al. 2010; Coen et al. 2018; McClung and Mass 2020).

During the past decade, wind-driven wildfires have caused numerous fatalities and substantial economic loss in central and northern California. The 2017 Tubbs Fire (the most damaging of the Wine Country Fires), the 2018 Camp Fire, and the 2020 North Complex Fires led to 122 deaths. The Tubbs Fire, the Camp Fire, and the 1970 Laguna Fire were initiated by failing electrical infrastructure during high winds, which also produced rapid fire spread (Keeley and Zedler 2009; Mass and Ovens 2019; Mass and Ovens 2020). The Camp Fire was the costliest insured environmental loss of 2018 globally at $12,500,000,000, even exceeding the cost of the 2017 Wine Country Fires the year before (Associated Press 2018; Löw 2019). The 2020 fire season led to the first recorded "megafire" in California history as the wind-driven August Complex Fire burned more than one million acres (Kaur 2020). With the exception of the 1970 Laguna Fire, the above-mentioned fires were considered Diablo-wind fires, associated with strong northeasterly winds over northern California (McClung and Mass 2020).

Major wind-driven fires in southern California are often associated with northeasterly Santa Ana winds which are also strong and dry. Examples of wildfires resulting from Santa Ana winds include the 1889 fire season, the 1970 Laguna Fire, several fires during the 2003 and 2007 fire seasons, and the 2017 Thomas Fire (Mensing et al. 1999; Keeley and Fotheringham 2003; Keeley et al. 2004; Keeley et al. 2009; Keeley and Zedler 2009; Addison and Oommen 2020). The 1889 fires were associated with strong winds and large burned areas not matched until the past decade (Keeley et al. 2004). The 2003 Cedar Fire was the largest on record at the time of burning and was a wind-driven event (Mensing et al. 1999; Keeley and Fotheringham 2003; Keeley et al. 2004). In 2007, seven lives were lost in large southern California wildfires that produced $1.8

billion in property loss (Karter 2008; Keeley et al. 2009). The December 2017 Thomas Fire, also the largest fire at the time of occurrence, was associated with strong, dry winds and resulted in nearly two-dozen deaths and approximately $207 million in damage (Addison and Oommen 2020).

1.3 Background: wind driven fire in California

As described above, the fire characteristics of grassland/chaparral and forested regions differ, with varying impacts of meteorological parameters such as wind, temperature, and dryness (Schoennagel et al. 2004; Scott and Burgan 2005; Keeley and Syphard 2019). California's expanding human development interacts with its climate and frequently dry surface fuels to make the state a favorable location for wildfire occurrence (Pagni 1993; Skinner and Chang 1996; Field and Jensen 2005; Hammer et al. 2007; Moritz et al. 2010; Coen et al. 2018; Radeloff et al. 2018; Syphard et al. 2019; McClung and Mass 2020).

1.3.1 *California's major ecological fuels*

California can be divided into "fuel-dominated" (generally forest) and "wind-dominated" (generally savanna) regimes (Keeley and Syphard 2019). Although the area burned in California is dominated by savanna/shrubland-dominated landscapes, extensive regions of the state are forested (Keeley and Syphard 2017; Schwartz and Syphard 2021). California typically experiences cool, moist winters that facilitate the annual growth of fast-growing savanna vegetation (defined here as chaparral/grassland/shrubland—Friedl et al. 2002) (Steel et al. 2015). In contrast, California's summers are generally hot and dry, which rapidly desiccates fast-drying savanna fuels and more slowly dries forest environments (Steel et al. 2015).

The wildfire characteristics of savanna and forest fuels can differ in important ways. Savanna landcover, including grasses, bushes and small vegetation, dries more rapidly and is

more easily ignited than forest. Savanna fire intensity is characterized by the high energy release potential of its fuels and may foster particularly fast-moving wildfires (Scott and Burgan 2005). Timber fires have the potential for higher emissions due to the large fuel density and high carbon content of the fuels. However, it is more difficult to burn live timber than savanna and particularly difficult to achieve tree mortality because of the relatively thick bark of trees, generally necessitating a crown fire to initiate tree death (Lawes et al. 2011).

Furthermore, the replacement of native vegetation by flammable invasive species has enhanced the vulnerability of California's savanna regions to wildfire (Keeley et al. 2011). Defining "interface WUI" as urban areas adjacent to wildland vegetation (but without containing such vegetation) and "intermix WUI" as urban areas mixed with wildland ones, it is found that most California structure damage occurs in interface WUI (Kramer et al. 2019). Additionally, the built environment may contain fuels that burn at higher intensity than the natural vegetation would (Kramer et al. 2019). Finally, at the interface between savanna and forest ecosystems, fires may ignite in savanna and spread to forest (Bond and Midgley 1995; Syphard and Keeley 2015; Mass and Ovens 2020).

Examining the varied impacts of meteorology on wildfires burning in differing naturally occurring fuel types in California is a major goal of this thesis.

1.3.2 *Fuel drying*

Dry conditions (low humidity, large vapor pressure deficit—VPD) contribute to California wildfires. Dry conditions reduce the fuel moisture content of vegetation and thus increase their flammability (Chandler 1983, Agee 1993; Westerling et al. 2004; Liu et al. 2020; Smith et al. 2018). At the peak of the fire season, the fuel moisture content (percentage of water in a plant) of even live timber can dip below the threshold "moisture of extinction," below which

a flame may be sustained on a plant (Chandler 1983; Agee 1993). Dead fuels are characterized by low moisture content that is controlled by surrounding environmental conditions[4] (Finney 1998; Matthews and Matthews 2013). Dead fuels are classified by the time required for fuel moisture content to reach two-thirds of the value consistent with equilibrium with the surrounding environment. This time lag is dependent on the fuel's diameter: 1-h fuels are under ¼" in diameter, 10-h fuels are between ¼" to 1", 100-h fuels are between 1" to 3", and 1000-hour fuels are between 3" to 8". Grasses behave similarly to dead fuels once approximately 80% cured[5], a desiccating process that occurs seasonally during an herbaceous plant's lifetime (Scott and Burgan 2005). Once herbaceous plants are 60% cured, rainfall will not cause the plant to green up again[5]. Although precipitation or dew will not cause green up in such a circumstance, the moisture can reduce grass flammability; however, this reduction in fire potential only lasts a few hours given sufficiently dry conditions (Bradstock et al. 2012).

1.3.3 *California's dry winds*

Strong winds influence fires as well. Wind influences fire spread rate by both advecting superheated gas and spotting, in which strong, turbulent winds loft firebrands ahead of the flame front, initiating new fires ahead (Koo et al. 2010; Fernandez-Pello 2017). Wind may also facilitate the drying of fuel or lead to fire ignition, such as with failing electrical infrastructure or when trees fall on powerlines (McClung and Mass 2020). Wind and humidity are not independent, especially in the presence of topography where strong, dry downslope flow can occur. The peak of the fire season in California encompasses late summer and fall, a particularly dangerous time, since it follows the extended California dry season and is often a period of

[4] https://www.wfas.net/index.php/dead-fuel-moisture-moisture--drought-38
[5] https://www.weather.gov/media/dmx/CuringGuide2010_DMX.pdf

strong, dry, downslope winds associated with building high pressure over the intermountain West resulting from the cooling of the continental interior.

The surface synoptic-scale winds associated with California fires are usually from an easterly direction and thus represent offshore-directed flow (Bowden et al. 1974; Westerling et al. 2004; Hughes and Hall 2010; Abatzoglou et al. 2013; Cao and Fovell 2016; Rolinski et al. 2016; Bowers 2018; Rolinski et al. 2019; McClung and Mass 2020). These winds are often caused by surface high pressure in the Northwest interior and Great Basin following southward pushes of lower-tropospheric cool air into the intermountain west (Bowden et al. 1974; Hughes and Hall 2010; Cao and Fovell 2016; McClung and Mass 2020). The resulting strong near-surface pressure gradient (from high pressure in the Great Basin to low pressure over the West Coast) forces air over the Sierra Nevada, Cascades, and coastal terrain in the coastal portions of the western U.S. Although winds are accelerated westward by the strong regional pressure gradient, mountain wave structures can also form if the stability and wind conditions upstream allow mountain wave amplification, resulting in enhanced winds on the leeward sides of regional terrain barriers (Corby 1954; Durran 1990; Abatzoglou et al. 2013). Such downslope wind acceleration can produce spatial variation in wind strength (Cao and Fovell 2016; Rolinski et al. 2016).

The easterly winds associated with wildfire in California are generally dry as they originate over the dry continental interior. The easterly flow may dry further as it moves across regional terrain. First, if the air mass begins with sufficient moisture, much of this moisture may be lost in an irreversible manner as the air mass rises over the eastern slopes of the Sierra Nevada, cools, reaches its dew point, condenses water, and precipitates. Second, once the air crests the Sierra Nevadas and descends, it warms adiabatically from compression, reducing

relative humidity (Holton 1992). Additionally, the region east of California is generally at higher elevation than much of California itself. Depending on the initiating air mass's location, the air may start from higher elevation and descend monotonically, thus increasing its warmth and dryness monotonically.

Climatologically, dry and offshore directed flow over California tends to occur from fall through spring. These conditions often follow the southeastward passage of upper level troughs, and the cold air and associated surface highs that follow (Smith et al. 2018; Keeley and Syphard 2019; Liu et al. 2020; McClung and Mass 2020). In summer, a strong coastal pressure gradient may occur but is associated with onshore (westerly flow) between the typical offshore Pacific high and thermal trough over western California. Such onshore flow brings low-level moisture and higher relative humidity, which work against wildfire initiation and spread, even under windy conditions (Edinger 1963; Stephens 1968; Mass et al. 1986). Wildfire events have occasionally occurred during the generally moister winter period, when strong offshore flow has occurred such as during the aforementioned December 2017 Thomas Fire (Shi et al. 2019). Although a limited number of California wildfire events have been associated with westerly winds or weak winds, easterly winds tend to dominate most notable California wildfire events (Routley 1992; Keeley and Zedler 2009).

1.3.4 *Review of meteorological fire indices*

Several fire weather condition metrics (or indices) have been developed that make use of humidity, wind, and other meteorological parameters. These indices include the Fosberg Fire Weather Index (FFWI; Fosberg 1978), the National Fire Danger Rating System (NFDRS; Bradshaw et al. 1984), the Forest Fire Weather Index (FWI; Van Wagner 1974), Fire Potential Index (FPI; Burgan et al. 1998), and the Red Flag condition index (Murdoch and Gitro 2010).

Beyond these metrics, research groups have created other indices (e.g. Rolinski et al. 2016; Srock et al. 2018; McClung and Mass 2020).

Recent research has suggested that combining dryness and wind speed may provide useful wildfire guidance (e.g., Sharples et al. 2009a; Sharples et al. 2009b). For example, the Hot-Dry-Windy (HDW) index, which combines wind speed and vapor pressure deficit (VPD), enables skillful prediction of fire danger at short time lags (Srock et al. 2018). VPD is used rather than relative humidity (RH) because VPD is better related to the total amount of evaporation that can occur at a certain temperature, especially in vegetation (Johnston 1919; Anderson 1936; Seager et al. 2015; Srock et al. 2018; Williams et al. 2019; Parks and Abatzoglou 2020). One drawback of HDW is that the combination of VPD and wind speed does not inform about their individual contributions to the criterion, since high values of HDW may be due to high winds, dryness, or both. Other fire indices also combine dryness and winds, such as the Burning Index (part of the NFDRS), which combines a spread component dependent on wind speed and an Energy Release Component (ERC) related to the available potential energy resident in the fuels, which is dependent on drying conditions (Heinsch et al. 2017).

1.4 Research questions considered in this thesis

Prior research has examined the relationship between wildfires, wind, or humidity over the aggregate western U.S. (Abatzoglou and Kolden 2013; Abatzoglou and Williams 2016; Jones 2017; Parks and Abatzoglou 2020, Keeley and Syphard 2017; Williams et al. 2019). However, such geographically broad views often neglect local fuels and topography, which can be important modulators of wildfire potential (Rothermel 1972; Keeley and Syphard 2019; Syphard et al. 2019, O'Brien et al. 2018). Furthermore, such studies often do not consider regional variations in atmospheric conditions that can greatly modulate fire initiation and growth. Such

geographic variations are important in California, where a heterogeneous distribution of savanna and forests of California interacts with large mesoscale meteorological contrasts. To examine such issues of spatially varying fuels and meteorology, this thesis considers several major questions regarding the complex nature of California wildfires, including:

- What are the historical spatial and temporal characteristics of California wildfire emissions in the major fuels categories (savanna and forest)?
- How do fire-relevant weather conditions such as day-of-fire dryness, antecedent dryness, and wind affect fire emissions in savanna and forest?
- What are the spatial patterns of the meteorological forcings associated with varying amounts of wildfire emissions?

This thesis is organized as follows. Chapter 2 describes the fire emissions dataset and discusses the spatial and temporal climatology of California fires, including their evolution in different fuels ecosystems. In Chapter 3, the meteorological dataset is described and the relationship between weather and emissions is examined. In Chapter 4 we composite the fires and meteorology by emissions and describe the aggregate meteorological conditions associated with fires of varying severity. In Chapter 5 we present the spatially varying meteorology associated with the different emissions levels described in Chapter 4. Finally, in Chapter 6 we present our conclusions.

Chapter 2

Climatology of wildfire emissions across California

In this thesis, we use the Global Fire Emissions Database, Version 4.1 (GFEDv4, also referred to as GFED). The GFED dataset includes gridded fuel and fire emissions data, both derived from Terra and Aqua satellite Moderate Resolution Imaging Spectroradiometer (MODIS) imagery (Mu et al. 2011; Giglio et al. 2013; van der Werf et al. 2017; Randerson et al. 2018). GFED data was available daily from January 2003 through October 2020, with a horizontal grid spacing of 0.25º. Carbon emissions data provides information on the initiation and severity (ecological consequence influenced by spread and intensity) of fires, with higher emissions associated with larger amounts of burnt fuels and more complete combustion. Carbon emissions in the GFED data are also affected by fuel type, surface temperature, solar radiation, and soil moisture. In this thesis, "a fire" refers to a GFED grid cell with greater than zero emissions. The area burned by large fires can span an entire grid cell or multiple grid cells, and multiple fires can also occur in a single grid cell. Continuous emissions in a single grid cell are considered "one fire" for the purposes of this thesis.

The GFED dataset also records the percentage of varying land covers (fuel types) within each grid cell (Figure 1). In California, the three major land cover types are *savanna* (described as "savanna, grassland, or shrubland" in the MODIS land cover products—Friedl et al. 2002), *forest* (temperate extratropical forest distinct from boreal forest as described in Akagi et al. 2011), and *agriculture*. Most savanna grid cells contain no temperate forest, and most forest grid cells contain no savanna. However, there are some mixed grid cells with both savanna and forest, which are identified as either savanna or forest if 60% of the cell is of a single type; otherwise, they are discarded. Two additional land covers are shown in Figure 1, non-vegetated and urban, with non-vegetated analogous to "bare ground" in Scott and Burgan 2005. Although agricultural, non-

vegetated, and urban areas theoretically do not allow fire spread, sub-grid scale fuels may exist, so emissions from these regions are included in this thesis.

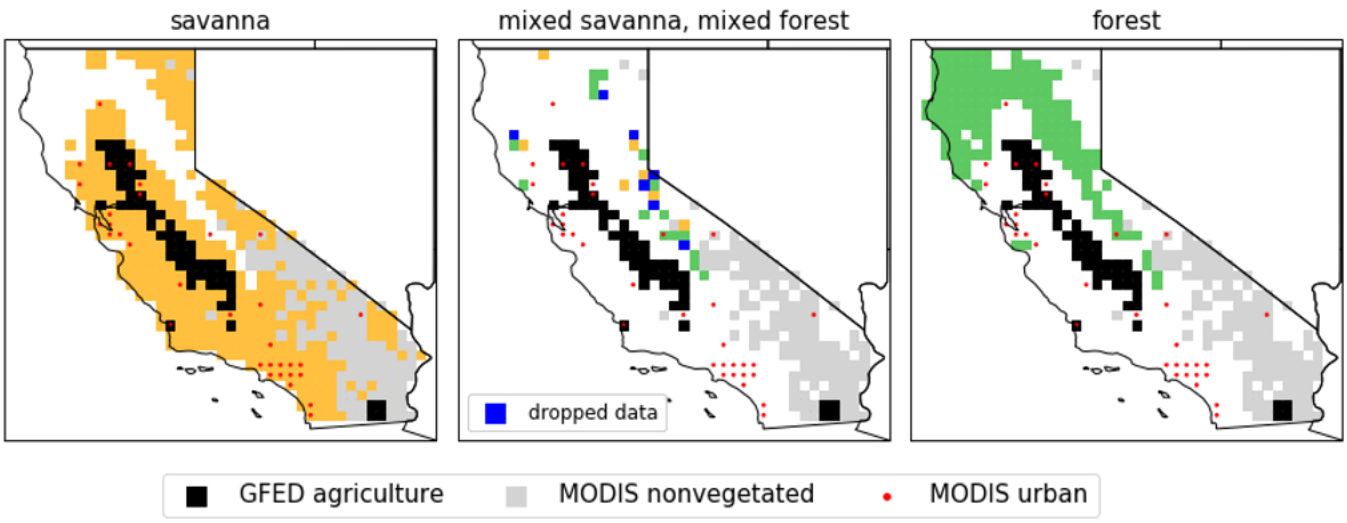

Figure 1: Distribution of savanna, mixed savanna/forest, and forest grid cells, as well as cells that are predominantly (75%) agriculture or non-vegetated. Urban areas are indicated by dots. Data discarded based on land cover percentages is shown in blue in the central figure.

To illustrate the application of the GFED dataset for regional wildfire analysis, Figure 2 displays the monthly carbon emissions across California savanna and forest for the 2003-2020 period. Emissions are highest during the late summer to early fall in both savanna and forest and appear to increase over time, with 2020 possessing peak or near peak emissions in both ecosystems. August is generally the month of the highest emissions for both fuels. Savanna emissions have more intra-annual variability than forest and span a wider range of months, starting earlier and often extending later into the autumn. The greater seasonal extent of wildfires in savanna is likely due to its small diameter fuels drying more quickly than large diameter timber, both earlier in the year and after autumn rain. Dead fuels, such as cured seasonal grasses, are more prevalent in savanna environments. Forest emissions possess greater inter-annual variability, likely

due to the relative difficulty in igniting and sustaining fire in forest, while having a larger amount of carbon available to burn than savanna when fires do occur. Emissions maxima in forest emissions are generally higher than those of savanna, although more area is burned in savanna/shrubland (Keeley and Syphard 2017).

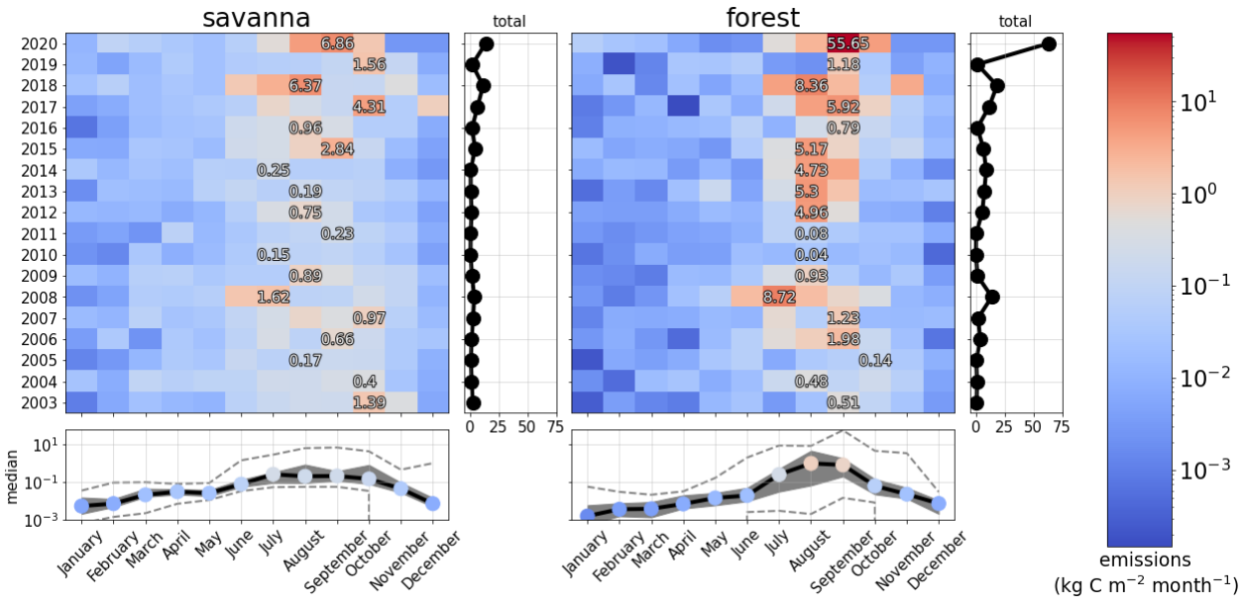

Figure 2: Monthly emissions of carbon (kg C m^{-2} $month^{-1}$, colors) in California's savanna and forest for 2003-2020. The annual totals and monthly medians are displayed for both fuels. The gray areas in the lower panels define the 25th and 75th percentiles of emissions, while the dashed lines indicate the maximum and minimum yearly values.

The spatial characteristics and seasonality of California wildfire emissions are illustrated in

Figure 3.

Figure 3a shows the month of maximum fire frequency of any emissions level (colors) and the number of days of fires at each point (indicated by size) for 2003 through 2020. Fires are most

frequent in the Central Valley of California due to agricultural burns. Most agricultural burns are small and take place early in the year (March-April) when wildfires are infrequent.

Figure 3b, which provides emissions amounts and the month of maximum emissions, indicates that wildfires with larger emissions (bigger markers) are generally observed later in the year (June-October), typically on mountain slopes and northern California forests.

Figure 3 also shows the spatial distributions of wildfires with maximum daily emissions exceeding 10, 50, and 100 g C m-2 24 hr-1, respectively. Higher emission fires are mainly found over the terrain of central and northern California, with the fire frequency in southern California rapidly declining as emissions increase. This decline in emissions over southern California reflects the low carbon content of the savanna fuels that dominate the southern portion of the state and the lower severity at which they typically burn.

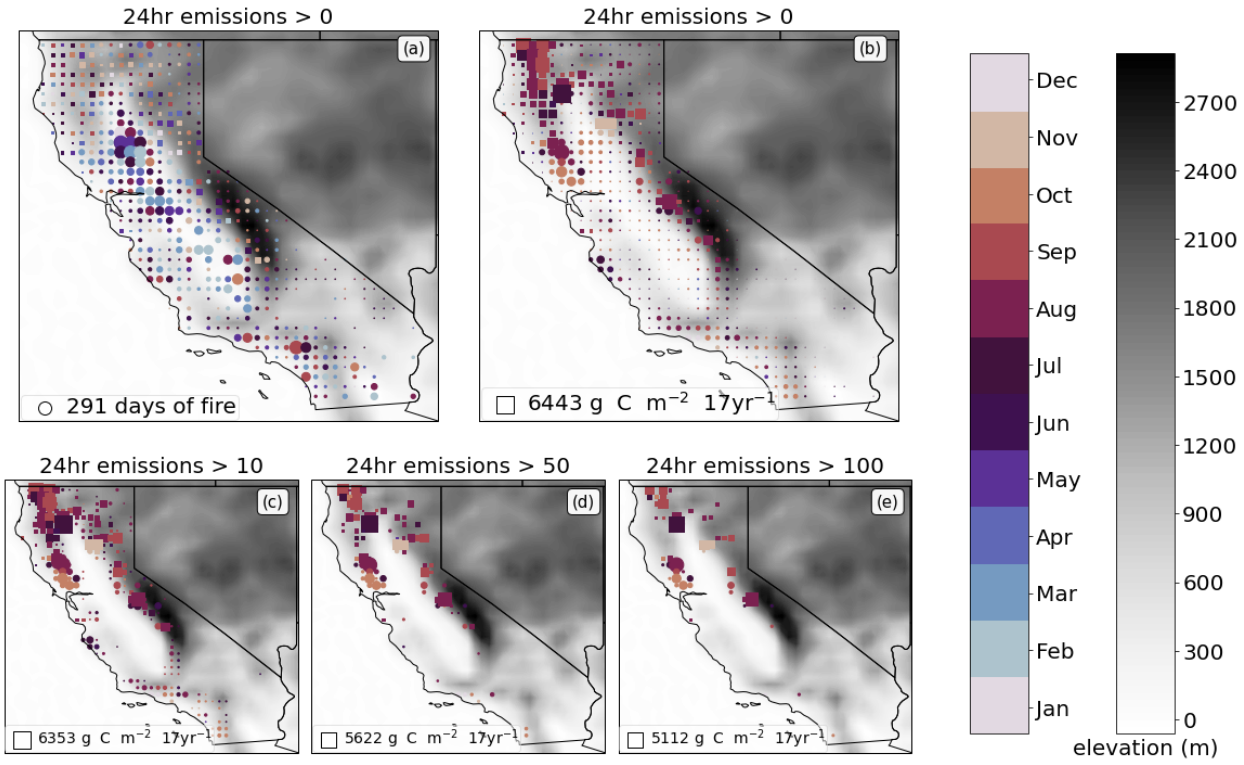

Figure 3: Wildfire emissions across California (squares: forest, circles: savanna). a) The calendar month (indicated by color) with the greatest number of wildfires, with the marker size indicating the number of fires. b) The calendar month (indicated by color) of greatest wildfire emissions, with the total emissions indicated by symbol size. c, d, e) as in *b* but for wildfires with maximum daily emissions exceeding 10, 50, and 100 g C m^{-2} $24hr^{-1}$, respectively.

The differences in emissions between savanna and forest areas are further explored in Figure 4, which presents cumulative frequency histograms as a function of emissions for savanna and forest for the entire state of California for the 2003-2020 period. The emissions distribution for savanna is dominated by small fires, with only 1.1% of the fires emitting more than 10 g C m^{-2} $24hr^{-1}$. In contrast, for forest areas, 11.8% of the fires emit 10 g C m^{-2} $24hr^{-1}$ or more. Considering both forest and savanna together, fire days with emissions greater than 10 g C m^{-2} 24 hr^{-1} make up approximately 4% of the overall days of fire but account for nearly 85% of the overall emissions. For the remainder of this thesis, emissions greater than 10 g C m^{-2} 24 hr^{-1} are considered "high emissions".

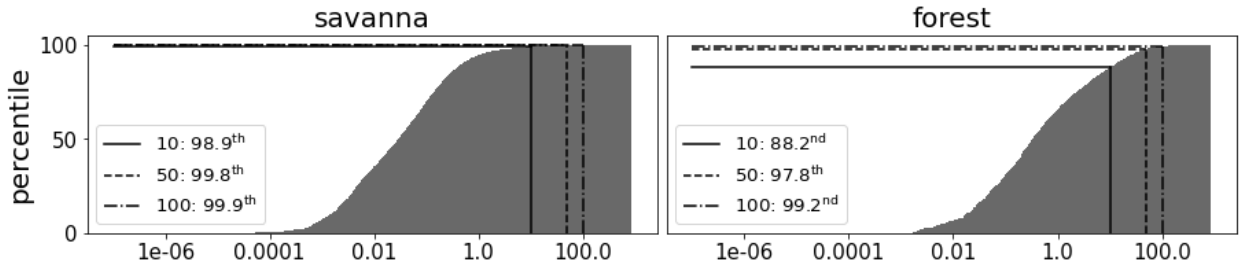

Figure 4: Cumulative histograms showing the percentiles of fires in savanna (left panel) and forest (right panel) fuels that reach the emissions thresholds of 10, 50, and 100 g C m^{-2} $24hr^{-1}$, respectively.

The GFED database can be used to examine the temporal evolution of savanna and forest fires over California. To illustrate, Figure 5 presents the evolution of individual savanna and forest fires that emitted more than 10 g C m^{-2} 24 hr^{-1} on at least one day. Most savanna fires begin with their highest emissions day or reach their highest emissions within the two ensuing days. Savanna wildfire emissions decline rapidly after they peak, and these fires rarely last more than 30 days (Figure 5a). In contrast, most forest fires last over a week and maintain higher emissions over an extended period, with some lasting more than 40 days (Figure 5b).

There is a subset of fires that show little growth for extended periods, with rapid increases in emissions weeks later. Such delayed growth is generally the result of renewed fire growth/spread forced by rapid acceleration of surface winds. Figure 5c illustrates the evolution of four such events in forest whose maxima occurred at least 30 days after ignition. For example, the Red Salmon Fire, which was ignited in late July 2020 (cyan color with peak emissions date of 2020-09-8 labeled), remained at a weak-to-moderate level of emissions for nearly a month, before exploding under the influence of very strong easterly winds (Abatzoglou et al. 2021). Other fires peaked multiple times during the weeks after ignition.

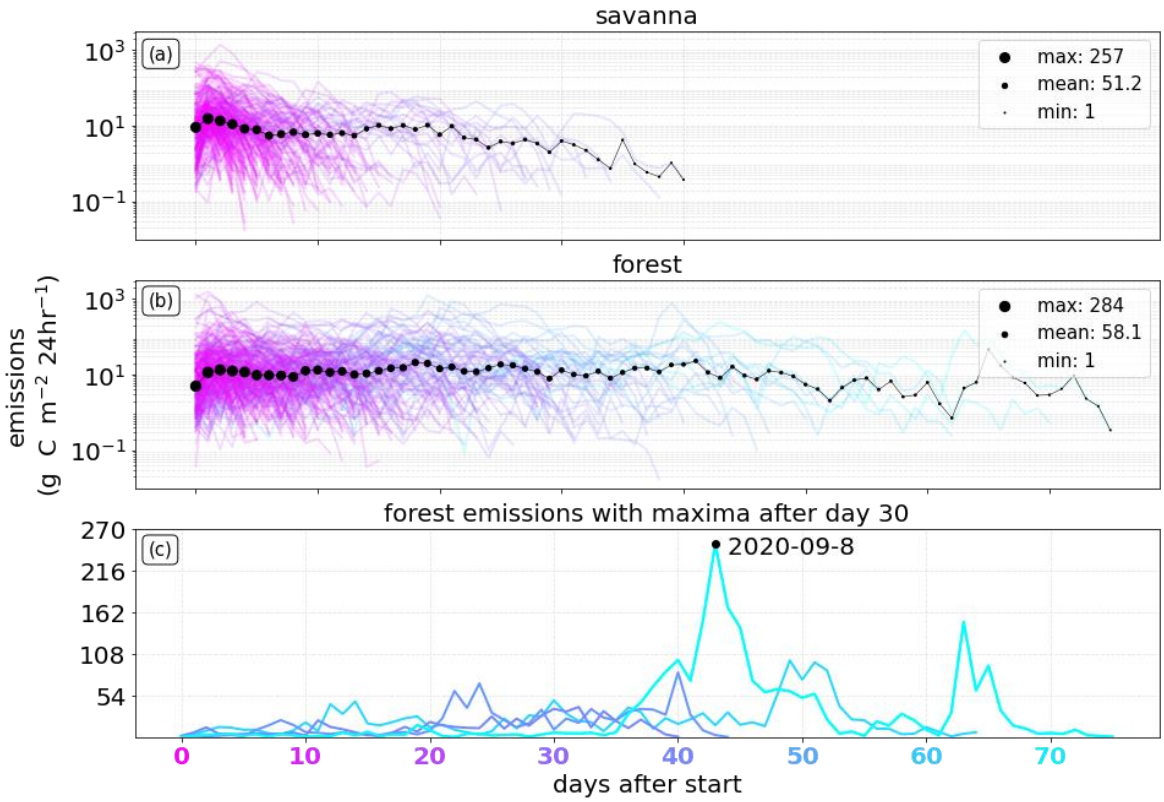

Figure 5: Wildfire emissions evolution for fires that emit greater than 10 g C m^{-2} 24 hr^{-1} on any day for savanna (a) and forest (b). The line color corresponds to the fire's eventual duration (colors shown on abscissa). c) The emission evolution of the four wildfires whose peak in emissions occurs after day 30.

Chapter 3

Meteorological conditions associated with California fire emissions

3.1 Meteorological dataset and validation

The meteorological data used in this thesis is from the European Center for Medium-Range Weather Forecasts (ECMWF) Reanalysis 5th Generation (ERA5), which assimilates weather observations using the ECMWF model over an extended period. ERA5-derived fields used in this work include temperature, relative humidity (RH), zonal and meridional components of wind, and geopotential height. We acquired these fields at hourly resolution from January 2003 through October 2020. The data has a horizontal grid spacing of 0.25^{o} (~30 km) and is vertically interpolated to 100-m increments.

Two meteorological parameters are considered in this thesis: wind speed and vapor pressure deficit (VPD), the difference between the saturation vapor pressure and actual vapor pressure. Large VPDs indicate enhanced drying conditions. In this thesis, the saturation vapor pressure for levels above terrain is calculated assuming dry adiabatic descent to the terrain level, with the actual vapor pressure assumed to be that of the original ERA level. This adjustment accounts for the drying of elevated air that is vertically mixed to the surface during turbulence or daytime convection (Srock et al. 2018). VPD is calculated daily and for the prior 30-days.

Compared to RH, VPD is better related to the evaporation from fuels than RH, and thus more useful for evaluating preconditioning of wildfires (Johnston 1919; Anderson 1936; Kucera 1954). To illustrate the value of VPD compared to RH during wildfire events, Figure 6 compares every 50th value of daily RH, VPD, and temperature in the 500-m layer over the surface from 2017 through 2020 for California. High VPD, and thus strong drying, is only observed during periods of low RH. However, low RH is sometimes observed during periods of near-zero VPD, a clear

problem for the use of RH in evaluating surface drying. Cumulative counts are also shown in Figure 6 for VPD. Roughly 70% of the VPD samples are less than 15 hPa.

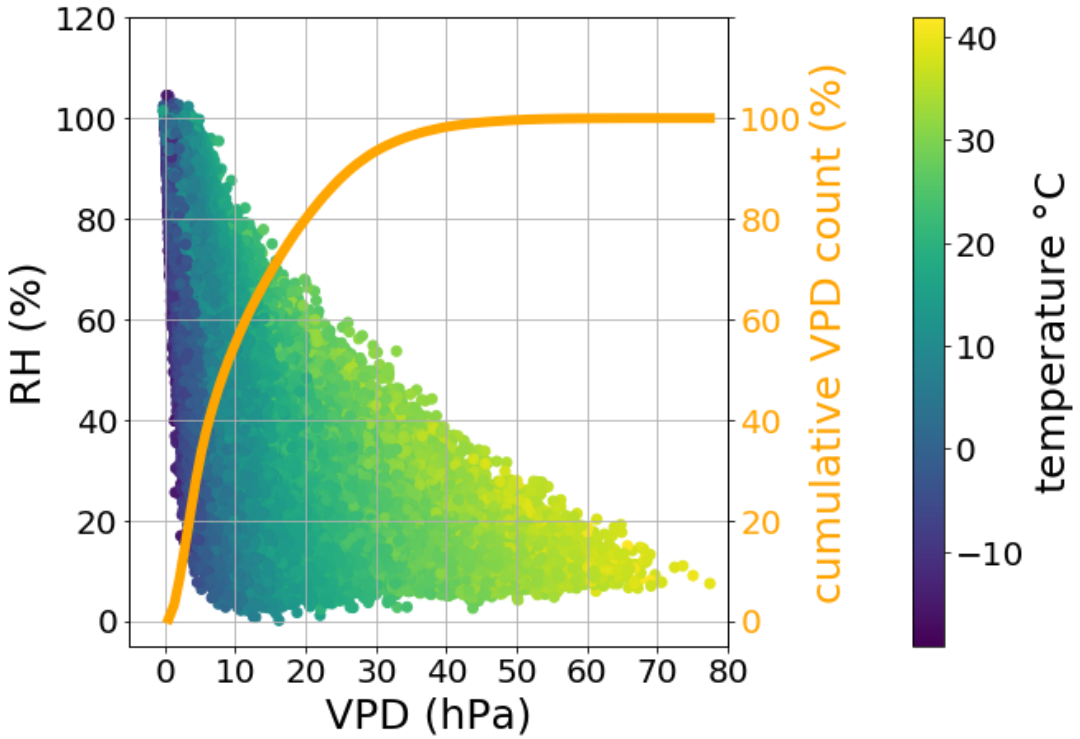

Figure 6: VPD compared to RH across the lowest 500 m of the atmosphere over California for 2017 through 2020. The color denotes the layer temperature (°C). Overlaid on the figure is a cumulative histogram of VPD (orange).

The ERA5 reanalysis is of sufficiently fine resolution (~30 km grid spacing) to resolve the broad characteristics of mesoscale features such as downslope wind events. To illustrate, ERA5 fields were used to describe conditions associated with the rapidly spreading 2018 Camp Fire (Figure 7). That fire was initiated on the morning of November 8th by a downslope, easterly wind event that damaged electrical infrastructure on the western slopes of the central Sierra Nevada (Mass and Ovens 2020). Maps of maximum winds and VPD in the lowest 500 m at 1400 UTC 8 November 2018 show strong winds above the western slopes of the Sierra Nevada and over the

coastal terrain, with higher VPD on the western Sierra Nevada slopes (Figure 7a, b). Vertical cross sections show that the ERA5 analysis defines downslope winds on the Sierra Nevada and internal gravity wave patterns in winds and VPD. These structures are consistent with higher-resolution model simulations of the event (Mass and Ovens 2020).

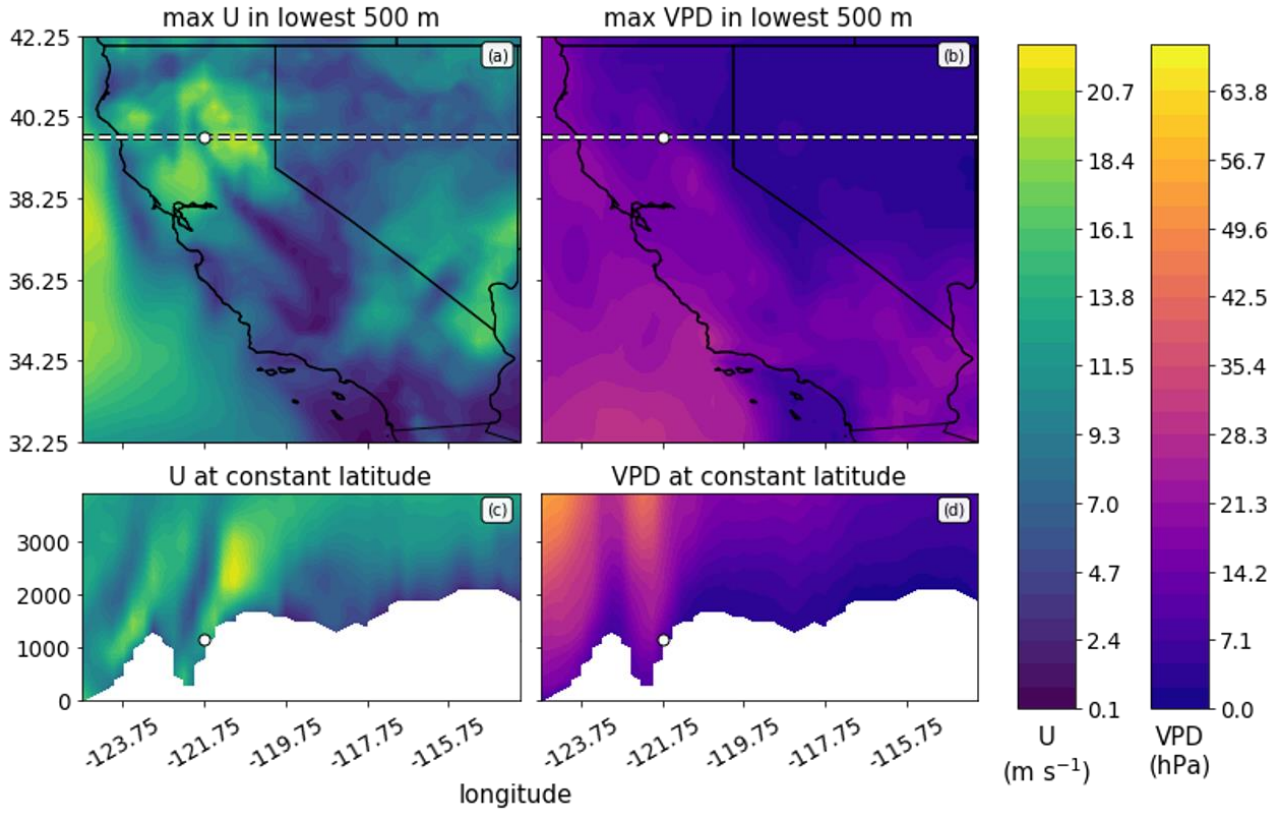

Figure 7: Winds (U, m s^{-1}; a, c) and VPD (hPa; b, d) associated with the 2018 Camp Fire. The fields are shown at 1400 UTC 08 November 2018, near the time of fire initiation.

3.2 Meteorological conditions during savanna and forest wildfires

To determine the meteorological conditions associated with varying wildfire emissions, hourly VPD and wind speed from the ERA5 dataset are compared with daily GFED emissions over the 18-year period of GFED observations. For each daily fire emission event in a GFED grid cell,

hourly VPD and wind speed during that day are recorded across the lowest 500 m above ground in the four horizontally adjacent ERA5 grid columns. The four surrounding columns are used because the ERA5 and GFED grids are offset by 0.125º in both horizontal directions. The wind speed and VPD for each emission point are calculated as follows: the wind speed is the maximum hourly wind speed recorded in the lowest 500 m and the VPD is the daily average of the hourly 500 m maximum VPDs. 30-day prior average VPD is calculated as well.

Maximum daily winds are used rather than the daily average because strong winds are critical for fire initiation and rapid fire spread. Such daily maximum winds in the ERA5 are generally close to the peak wind gusts observed at anemometers proximate to the wildfires. For example, the observed wind gusts for the Camp Fire (Jarbo Gap RAWS[6]: 17.9 m s^{-1} at 1413 UTC on 8 November 2018) are comparable to the ERA (18.2 m s^{-1} at 1400 UTC on that date). For the Wine Country Fires, the ERA daily maximum wind of 23.9 m s^{-1} for 9 October 2017 compares favorably to the Santa Rosa RAWS[7] observations (22.8 m s^{-1} at 0729 UTC on that date).

Daily emissions and associated meteorology for both savanna and forest wildfires are compared for all days with emissions, the maximum day of emissions of each fire, and the first day of emissions of each fire. Scatter diagrams of daily averaged VPD and daily maximum wind speed (Figure 8 left panels) indicate that high-emission savanna fires (red colors, emissions above 10 g C m^{-2} $24hr^{-1}$) for all days and maximum emissions days are mainly limited to periods with VPD greater than 15 hPa. In forest, high emission fires for all days and maximum emission days are predominantly associated with daily VPDs greater than 10 hPa. The first days of fires require slightly higher dryness in both fuel categories. To explore the potential impacts of antecedent conditions, daily VPD is replaced with VPD averaged over the preceding 30 days (right panels).

[6] https://mesonet.agron.iastate.edu/sites/site.php?station=JBGC1&network=CA_DCP
[7] https://mesonet.agron.iastate.edu/sites/site.php?station=RSAC1&network=CA_DCP

In forest, a greater VPD is then needed for high emissions, with high emissions occurring above approximately 15 hPa. For savanna, the use of the 30-day prior VPD produces little change in the scatter diagram compared to using day-of values. Weak emissions fires can occur at high dryness (large VPD) and strong winds in both fuel types.

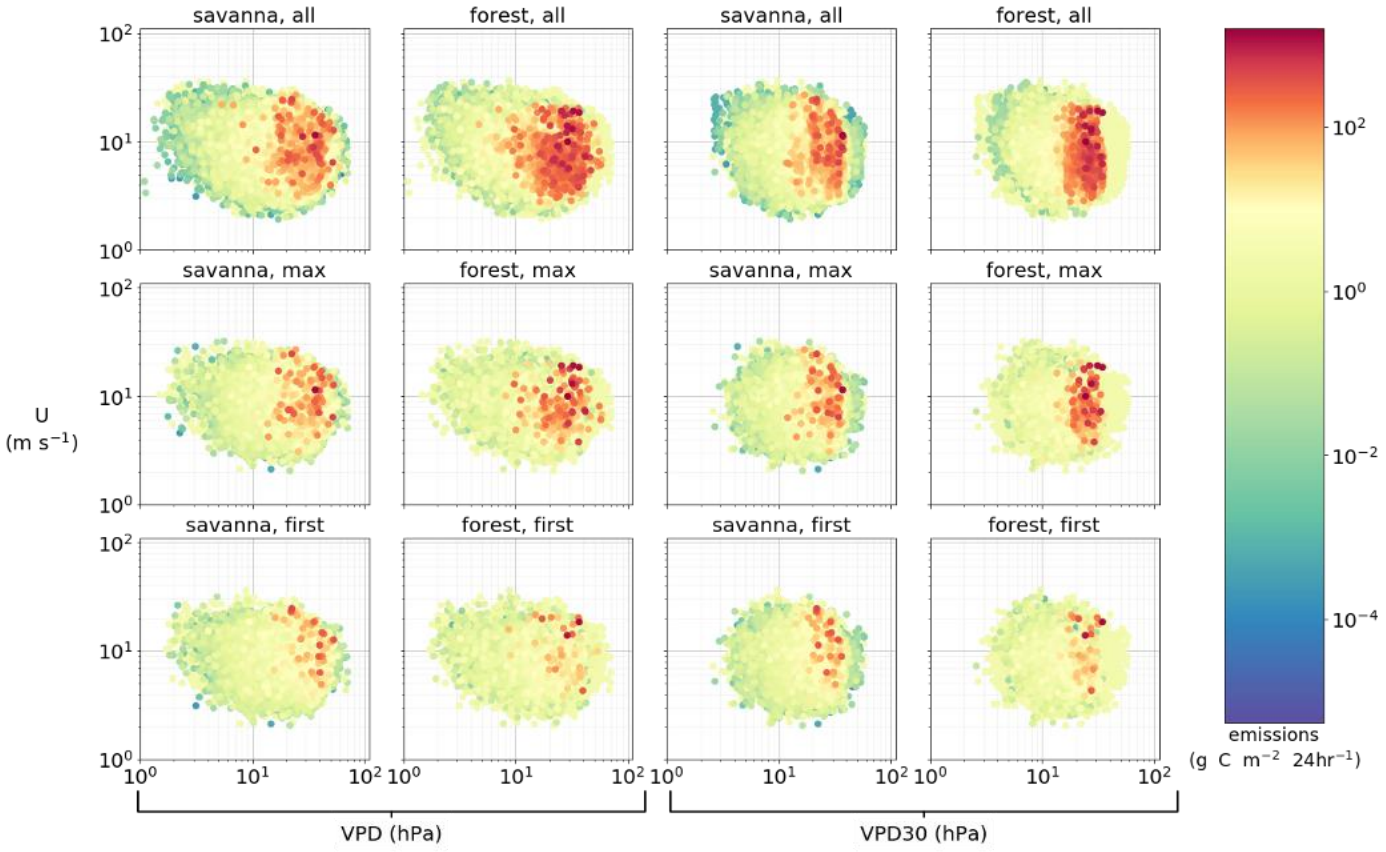

Figure 8: Emission amounts (colors), daily maximum wind (U, m s^{-1}), and average VPD (hPa, day-of: left panels; 30-day prior: right panels) are compared for all fire days, the maximum day of emissions, and the first fire day in savanna and forest.

Chapter 4

Aggregate meteorology and emissions

To gain further perspective into the relationship between emissions and near-surface meteorological conditions, the emissions were subdivided into small ranges (spans). Within these emissions spans, averages in the corresponding VPD and winds were computed, and their relationships with emissions explored.

4.1 The effect of VPD and wind speed on fire emissions

The relationship between average VPD and emissions is evaluated for both savanna and forest on all emission days, the maximum emission day, and the first emission day of each *fire* (Figure 9). For savanna, there is little trend in VPD for increases from weak to moderately high emissions (less than approximately 1 g C m^{-2} $24hr^{-1}$), but as emissions increase to higher levels (above 10 g C m^{-2} $24hr^{-1}$) there is a steady upward trend in VPD. For forest areas, there is a progressive increase in VPD from weak to high emissions. Above the high emissions threshold (10 g C m^{-2} $24hr^{-1}$) in both fuels, the trend flattens (for all days) and evinces more variability. There may be diminishing impacts of increasing dryness for high emissions wildfires. However, increases in the lower bound of the VPD spread (gray area) and the increase in the 25^{th} percentile of VPD imply that, for moderate and high emissions, elevated dryness may be a necessary condition.

Daily and antecedent (30-day prior) VPD were compared across emissions spans, with relatively small differences (figure not shown). For the maximum day and the first day of high emissions savanna fires, daily VPD is greater than antecedent VPD by around 5 hPa (the difference is significant at the 95% significance level). In forest, a smaller difference exists between dryness during emissions considering daily and 30-day antecedent VPD.

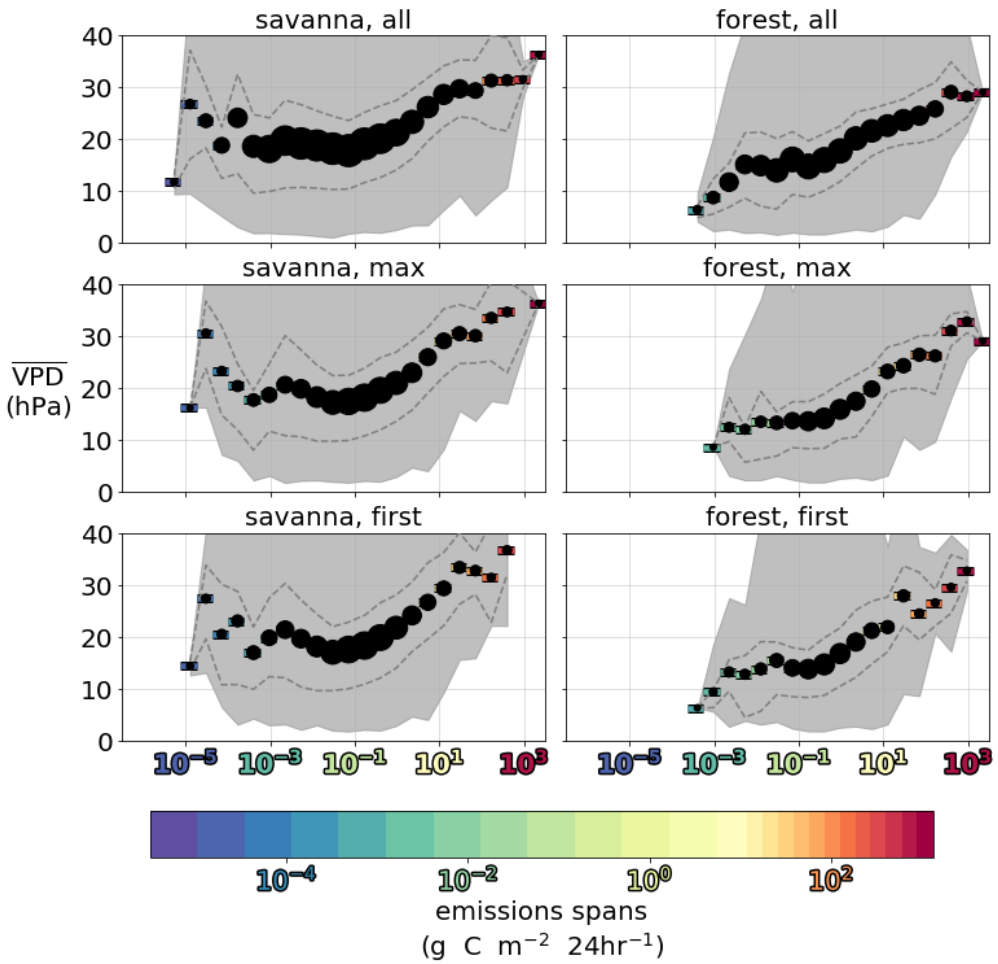

Figure 9: $\overline{VPD}$ (the overbar indicates averaged by emissions span, color coded) for all emissions days, the maximum day of emissions, and the first day of emission. The size of the symbol corresponds to the number of cases within each span (range: 9260, 1). The shaded gray area displays the spread (minimum to maximum), while the dashed lines display the 25th and 75th percentile for each span. Emission spans are indicated in the colorbar and shown behind each scatter point.

The relationship between the maximum daily winds and emissions is shown in Figure 10 for all days, the maximum emission days, and the first days of emission. For savanna, there is little trend in wind speed for emissions below 10 g C m^{-2} 24 hr^{-1}, but high emissions (above 10 g C m^{-2} 24 hr^{-1}) are associated with increasing winds. For forest fires, wind speed initially declines

with increasing emission, but wind speed increases for high emissions (above ~10-30 g C m^{-2} 24 hr^{-1}). Importantly, the largest increasing trend of winds with higher emissions occurs during the first day of fires in both fuels. This seems reasonable since strong winds are frequently associated with fire initiation and initial rapid wildfire growth.

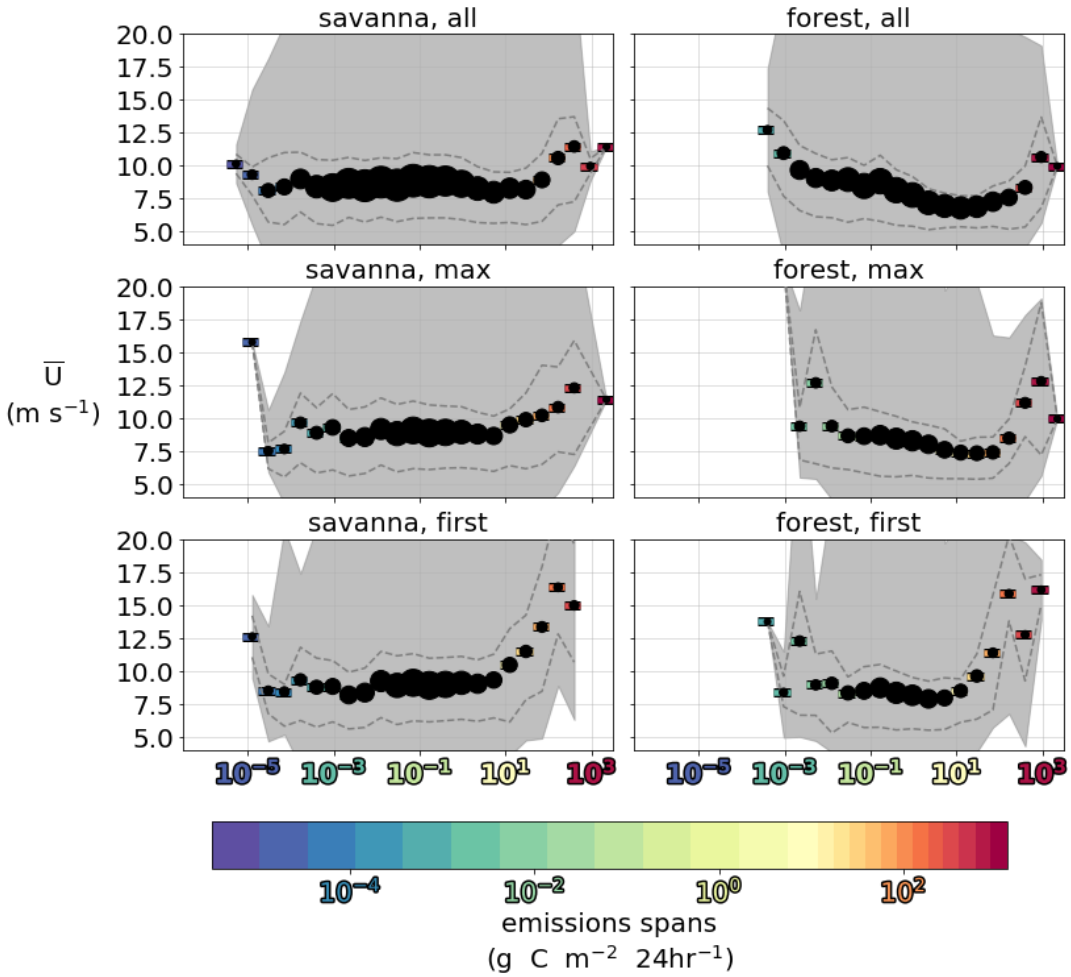

Figure 10: $\overline{U}$ (the overbar indicates averaged by emissions span, color coded) for all emissions days, the maximum day of emissions, and the first day of emission. The size of the symbol corresponds to the number of cases within each span (range: 1, 9260). The shaded gray area displays the spread (minimum to maximum), and the dashed lines display the 25th and 75th percentile for each span. Emission spans are indicated in the colorbar and shown behind each scatter point.

4.2 How unusual are the winds and VPD for varying emissions?

Another way of exploring the relationship between emissions and meteorology is to examine emissions as a function of the climatological percentiles of wind and VPD. Do high emissions require unusually strong meteorological forcing? To answer this question, we present various emissions spans as a function of the percentiles of wind and VPD for the 2003-2020 period (Figure 11). The percentiles are calculated as compared to the populations of similar fire days in similar fuels. The number of cases in each emissions span is shown by the symbol size.

For savanna, weak and moderate emissions (below ~10 g C m^{-2} 24 hr^{-1} respectively) are associated with winds near the 50th percentile. For VPD, there is a trend toward higher percentiles (from around 40th to 80th) for weak to moderate emissions (green to yellow). High emissions in savanna (yellow to red, above 10 g C m^{-2} 24hr^{-1}) are associated with both higher percentile strong winds and higher percentile VPD, with increasing emissions more correlated with wind speed increases. In forests, for weak-to-moderate emissions (below ~10 g C m^{-2} 24 hr^{-1}) winds decline and VPD increases for increasing emissions. As in savanna, this situation changes substantially for high emissions (yellow to red above 10 g C m^{-2} 24hr^{-1}), with winds increasing rapidly for higher emissions. At the highest emissions, both winds and VPD move towards the 90th percentile. The first days of forest fires require the greatest winds and dryness, possibly because the fire has not yet preconditioned surrounding fuels. In summary, for both savanna and forest, the highest emissions (dark orange, red) are found during periods of the most extreme simultaneous dryness and wind, as found for recent Oregon wildfire cases (Abatzoglou et al. 2021, Mass et al. 2021).

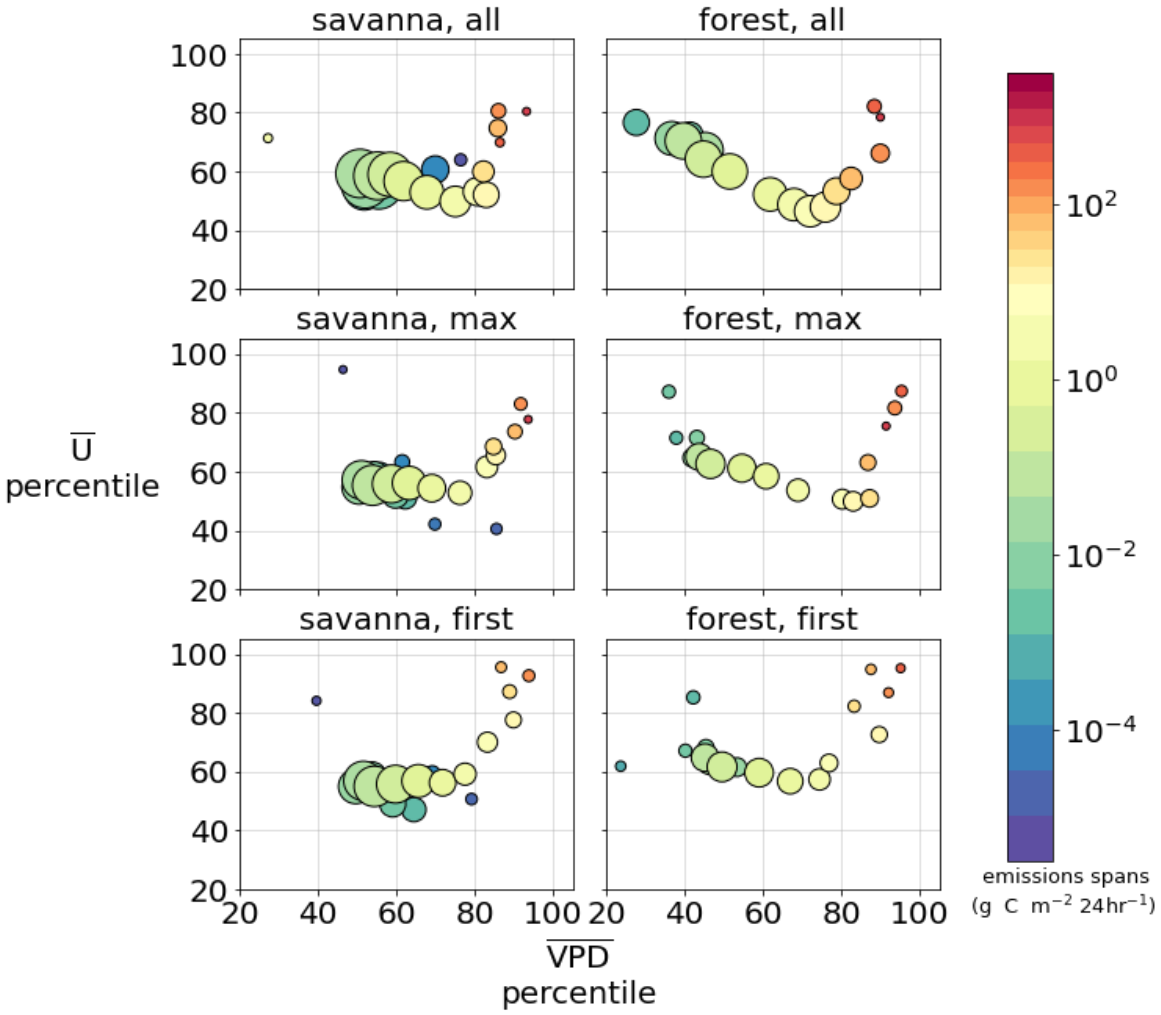

Figure 11: $\overline{VPD}$, $\overline{U}$, and emissions (colors) binned by emissions amount as a function of climatological (2003-2020) percentiles for all fire days, the day of maximum emissions, and the first day of fire in savanna and forest.

4.3 Seasonality of emissions

Although the seasonality of emissions was briefly addressed earlier (Figures 2, 3), in this section we describe the occurrence of varying levels of emissions as a function of the day of the year (Figure 12). We simplify the emissions spans into six bands: three weak-to-moderate bins (below 10 g C m^{-2} $24hr^{-1}$) and three high emissions bins (above 10 g C m^{-2} $24hr^{-1}$).

In both savanna and forests, weak-to-moderate emissions (under 10 g C m^{-2} $24hr^{-1}$) occur year-round; however, as emissions increase, the fires occur preferentially during the late summer and early autumn. There is a greater tendency for (relatively rare) high emission events to occur in autumn for forests, with a longer season for weak-to-moderate wildfires (green-yellow colors) in savanna.

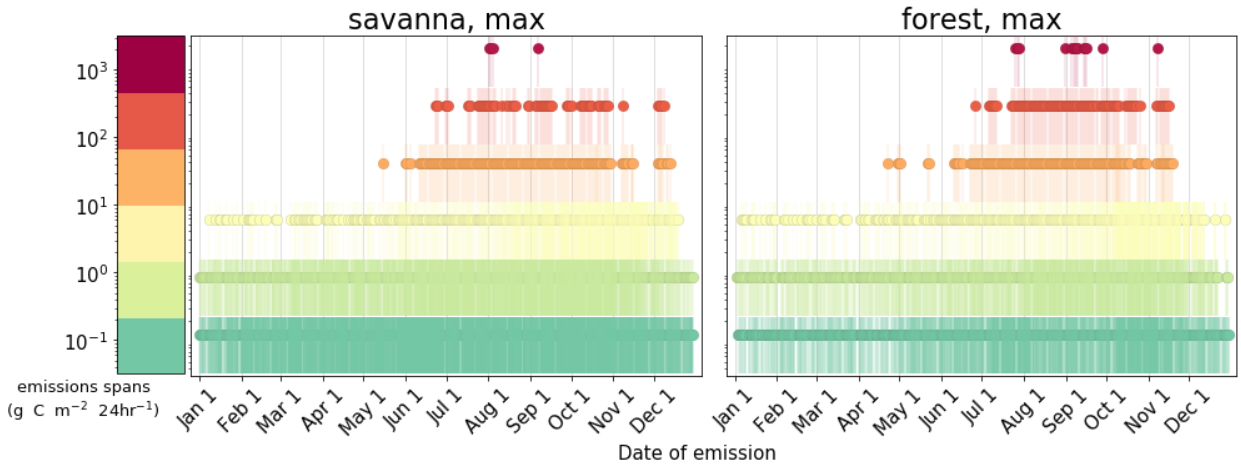

Figure 12: Annual variation for the maximum day of emissions in savanna and forest binned by emissions amounts. The transparency of the vertical lines is related to the frequency of such emissions on a particular day (more transparent: fewer cases).

Chapter 5

Regional spatial meteorology for varying savanna and forest emissions

To explore the spatial variability of the meteorological fields accompanying California wildfires, this section presents spatial maps that composite surface temperature and wind anomalies during the days of maximum emissions for various fuels and sub-regions of the state. These fields are shown as standardized anomalies, where the deviation from climatology is divided by the standard deviation over the climatological period (2003-2020). Both the climatology and standard deviations are computed for the 30-day period encompassing the event in question. State-wide meteorological composites are computed for the regions shown in Figure 13, which divide the state both spatially and by dominant surface fuel type. Emissions subregions qualitatively divide California into similar latitude regions and ecoregions, reflecting the heterogeneity of fuels and meteorology.

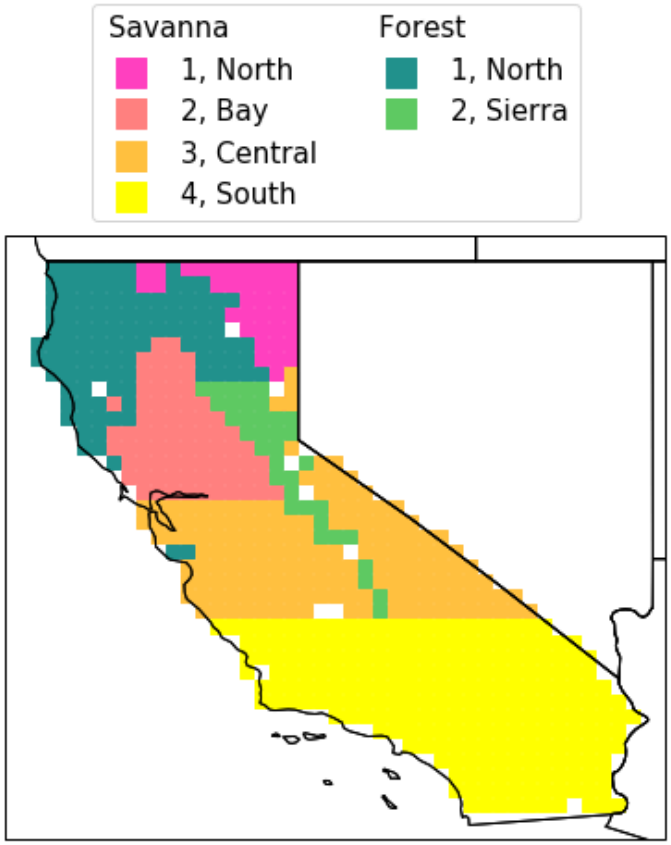

Figure 13: The four savanna regions (warm colors) and two forest regions (cool colors) considered in this thesis.

5.1 Regional spatial meteorology for forest fires

Starting with the North-Forest subregion, the area of highest emissions during the 2003-2020 period (Fig. 3), the temperature spatial composites (Figure 14a) indicate a weak warm anomaly over most of California for weak-to-moderate emissions, with highest temperatures over central/northern California. For higher emissions, a temperature gradient develops along the crest of the Sierra Nevada, with warmer temperatures to the west. For the highest emissions (greater than 464 g C m^{-2} $24hr^{-1}$), an intense warm anomaly develops over central and coastal California with colder than normal conditions over Nevada. Such interior cooling is consistent with cool, surface high-pressure systems moving into the intermountain basin, producing an offshore

pressure gradient that drives strong easterly downslope flow across the Sierra Nevada range (McClung and Mass 2020). The wind composites (Figure 14b) for the North-Forest subregion show lighter-to-normal winds across the domain during weak-to-moderate emissions fires. For higher emissions, the positive wind anomalies increase, especially across the North-Forest subregion and over southern California.

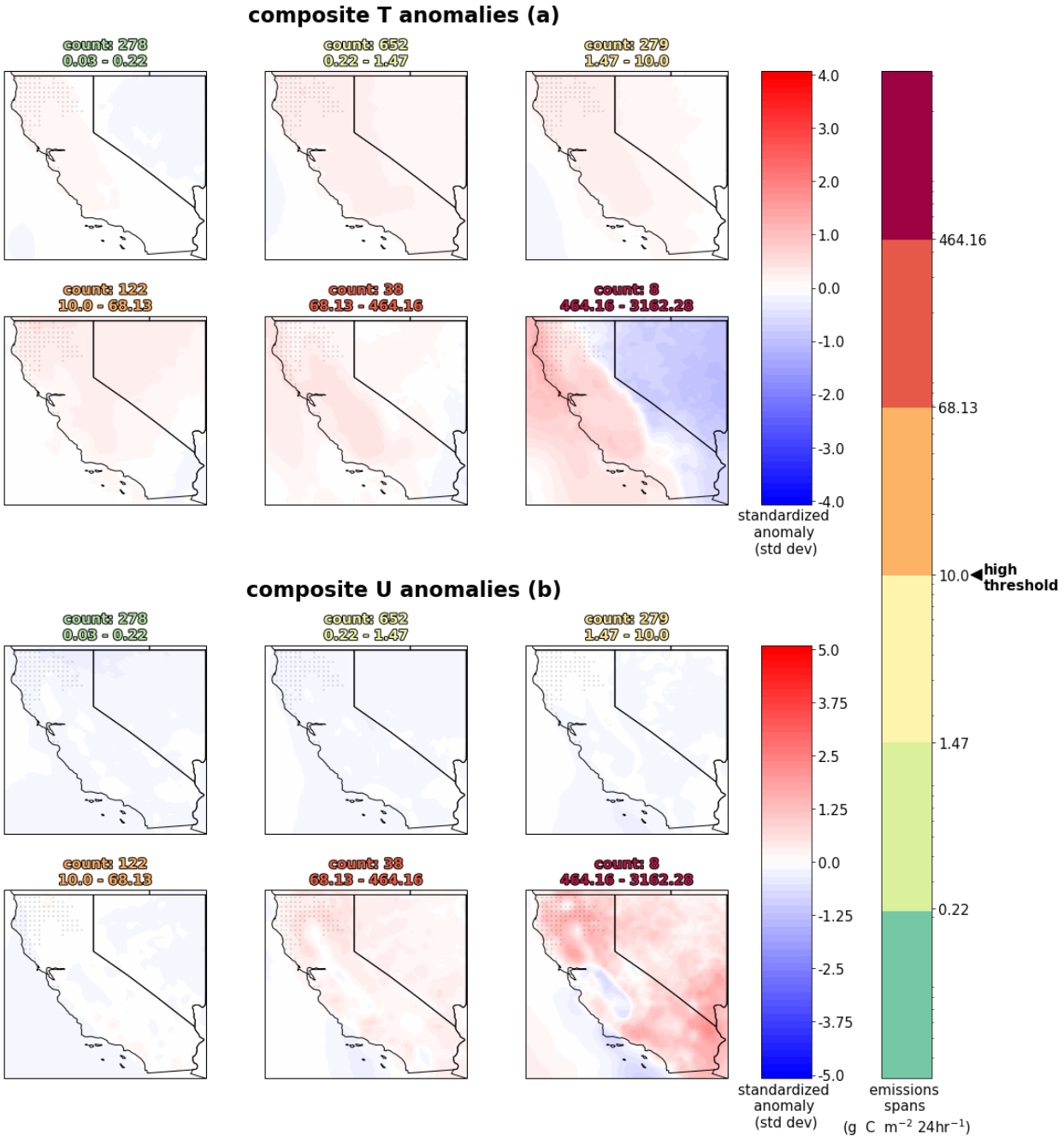

Figure 14: Standardized anomalies of surface temperature (a) and wind (b) (colors) for the maximum emissions day for the North-Forest subregion. The title of each subplot provides the number of days that make up each composite average and the emissions range. The light gray dots indicate the North-Forest subregion).

The temperature and wind composites for the Sierra-Forest subregion are similar to the North-Forest area and are not shown. The similarity in the composites is not surprising considering the relative proximity and identical fuel type compared to North-Forest. Small differences with North-Forest do exist, such as the shift of the largest temperature and wind anomalies towards the Sierra Nevada.

5.2 Regional spatial meteorology for savanna fires

For the savanna fuel type, we focus on the Bay-Savanna subregion, which includes 73 high-emissions fire days and several major fires such as the 2017 Wine Country Fires, and the South-Savanna subregion, which includes 66 high emissions fire days that include Santa Ana wildfires. The North-Savanna and Central-Savanna subregions contain fewer fires than the Bay subregion and are not shown for brevity.

For the Bay-Savanna subregion, weak-to-moderate emission events (below 10 g C m^{-2} $24hr^{-1}$), are associated with slightly warmer than normal conditions (Figure 15a). In contrast, the higher emissions events possess an increasingly strong temperature gradient across California and Nevada. For the highest emissions event, the coastal warming greatly intensifies, with strong cooling over northern California and Nevada.

Wind anomalies during weak-to-moderate Bay-Savanna fires are near zero across California (Figure 15b). For higher emissions, wind anomalies across the state become increasingly positive. Across the highest emissions cases, a complex pattern of strong wind anomalies is evident, with very strong winds over the coastal terrain north of the Bay Area and near the crest of the Sierra Nevada.

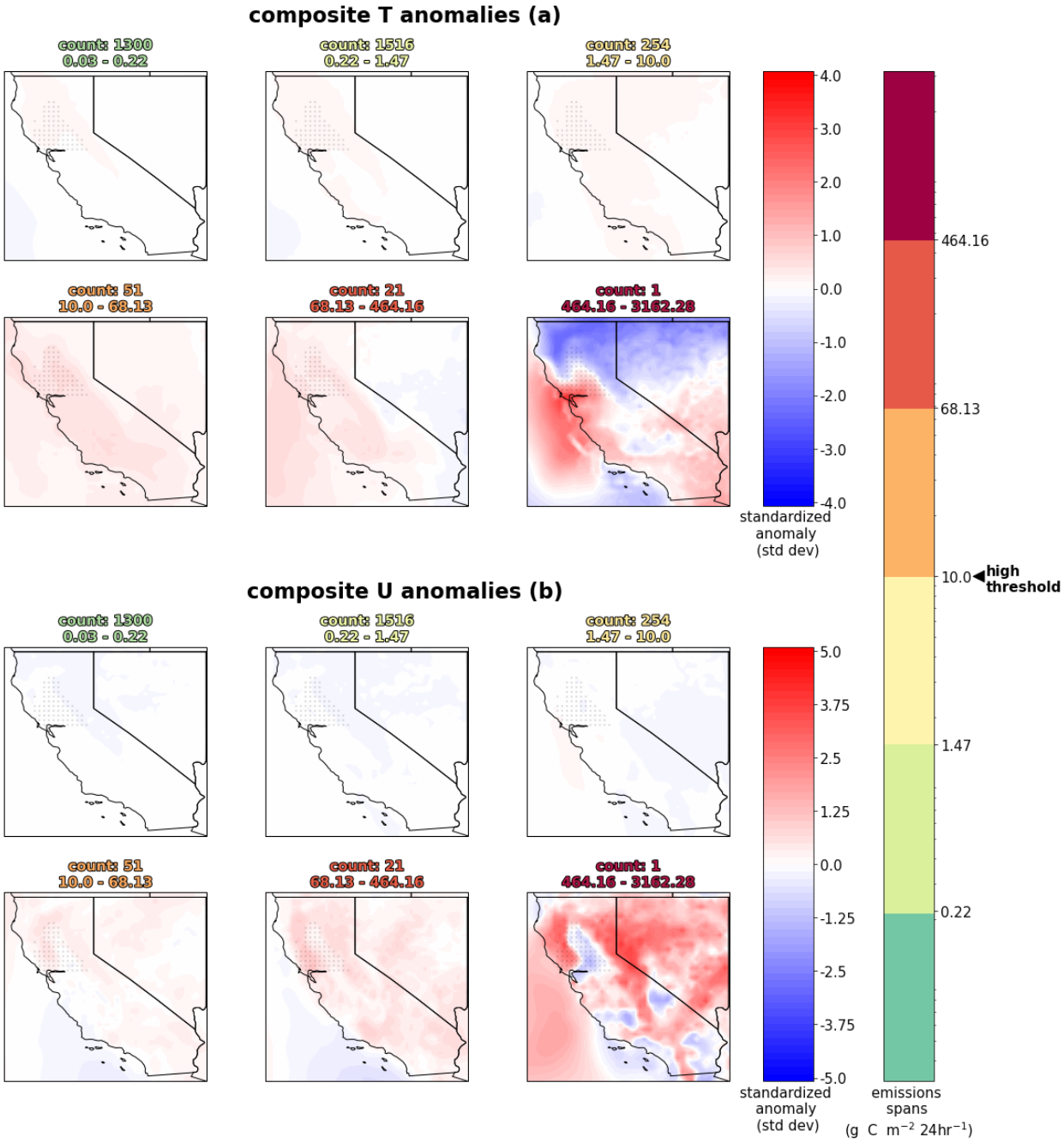

Figure 15: As Figure 14 but for the Bay-Savanna subregion.

Turning to the South-Savanna subregion (Figure 16), the temperature anomalies across California are very weak or even negative for the weak-to-moderate emission cases but become warmer than normal as emissions increase beyond moderate levels. For the largest emissions events (60-464 g C m^{-2} $24hr^{-1}$), warming increases along the coastal zone, with the interior of

California and Nevada becoming cooler than normal. As with forest, this surface temperature gradient is associated with cool, surface high pressure moving into the intermountain west (McClung and Mass 2020). For winds, South-Savanna events with weak-to-moderate emissions are associated with near-normal wind speeds (upper panels, Figure 16b). But as emissions over the subregion increase to higher values, the winds become much stronger over southern California, consistent with Santa Ana events (lower panels, Figure 16b). Winds also increase over the Sierra Nevada and the mountains of northern California.

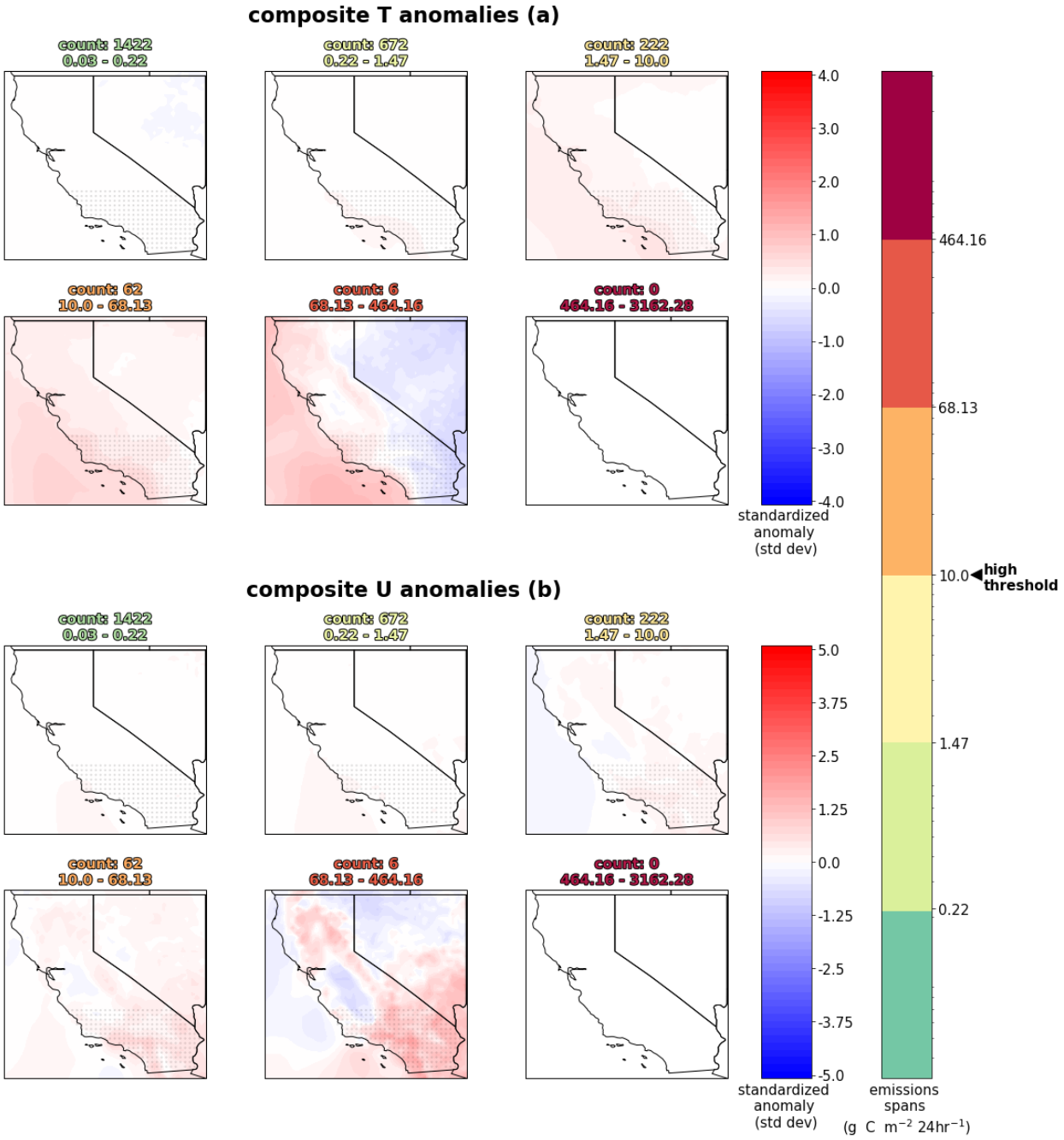

Figure 16: As Figure 14 but for the South-Savanna subregion.

Chapter 6
Conclusions

This thesis describes the climatology of emissions over California and evaluates the relationship between daily fire emissions and the regional meteorology for California's savanna and forest wildfires for 2003-2020. In this thesis, daily maximum wind, daily average vapor pressure deficient (VPD), and 30-day-prior average VPD are determined for wildfires of differing emissions across savanna and forest fuel types. A high-resolution comparison between wildfire emissions and meteorology is essential considering the heterogeneity of California's fuels and meteorology.

Two datasets are the foundations of this thesis. For emissions, we apply the Global Fire Emissions Database, Version 4.1 (GFED), which provides emissions data for a variety of fuel types on a 0.25-degree grid for 2003 through October 2020, while meteorological fields (temperature, relative humidity, winds) are acquired from the European Center for Medium-Range Weather Forecasts (ECMWF) Reanalysis 5th Generation (ERA5), which is available on 0.25-degree grids for the same period.

The emissions data reveals a strong seasonality for both savanna and forest wildfires, with greater seasonal spread for savanna and greater peak emissions for forest. Maps of emissions by season reveal that the greatest emissions are found during autumn over the northern forested areas of California, but with substantial emissions over the western slopes of the Sierra Nevada and the coastal mountains north of San Francisco. In contrast, the frequency of fires is more spatially uniform and dominated by savanna fires throughout the state and agricultural fires over the Central Valley. The cumulative histograms of wildfires frequency by emissions indicates that only 1.1% of the savanna fires emit more than 10 g C m^{-2} $24hr^{-1}$. In contrast, 11.8%

of the forest fires emit 10 g C m^{-2} $24hr^{-1}$ or more. Although forests burn less frequently than savanna, they possess far more fuel. Considering both savanna and forest areas, emission days greater than 10 g C m^{-2} $24hr^{-1}$ make up around 85% of the overall emissions.

Emissions, vapor pressure deficit (VPD), and wind speed are compared. We find that high emission (greater than 10 g C m^{-2} $24hr^{-1}$) savanna fires for all days and maximum emission days are mainly limited to periods with VPD greater than 15 hPa, while in forest, high emission fires for all days and maximum emission days are mainly limited to periods with daily VPDs greater than 10 hPa. In savanna, little change in these results is found using the VPD of the prior 30 days while in forest the high emissions threshold using the 30-day prior VPD increases to 15 hPa. Comparing savanna emissions with wind speed, we find little increase in VPD transitioning from weak to moderate emissions, followed by a steady upward trend in VPD for higher emissions. For forest areas, there is a progressive increase in VPD from low to high emissions. In both fuels, the VPD tends to level off for the highest emissions. Turning to winds, for savanna there is little to no trend in wind speed with weak-to-moderate emissions, but high emissions are associated with stronger winds. For forest fires, emissions initially decline as wind speed strengthens, but then increase with wind speed for higher emissions (above ~10-30 g C m^{-2} $24hr^{-1}$). The first days of fires require slightly higher VPDs (greater than 20 hPa) likely due to a lack of fuel preconditioning.

An important question relates to the relative frequency of the wind and dryness conditions associated with varying wildfire emissions in savanna and forest. This analysis finds that for savanna, weak and moderate emissions are associated with winds near the 50^{th} percentile. For moderate emissions, increasing emissions are associated with increasing VPD (from around the 45^{th} to 80^{th} percentile). Higher emissions in savanna are associated with both

strong winds and large VPD, with increasing emissions best related to increasing winds. In forest wildfires with weak-to-moderate emissions, winds decline (from around the 60th to 40th percentile) and VPD increases (up to around the 80th percentile) with increasing emissions. As in savanna, this situation changes substantially for the high emissions with winds increasing rapidly with emissions. The highest forest emissions are associated with wind speed and dryness around the 90th percentile. The highest emissions on the first days of forest fire require the most extreme combinations of strong winds and large dryness as expected from previous work on Oregon wildfires (Abatzoglou et al. 2021, Mass et al. 2021).

Next, this research examines the spatial variations in surface wind and temperature for savanna and forest wildfires in various portions of the state. For forest fires in mountainous northern California, there is a weak warm anomaly over most of California during weak-to-moderate emissions. For the highest emissions, a strong temperature gradient develops along the crest of the Sierra Nevada between an intensifying warm anomaly over central and coastal California and colder than normal conditions over Nevada. Such interior cooling is consistent with cool, surface high-pressure systems moving southward into the intermountain basin, producing an offshore pressure gradient that drives strong easterly downslope flow across the Sierra Nevada range (McClung and Mass 2020). Winds are light across the domain during weak-to-moderate emissions fires, but as fires increase in emissions, the wind anomalies first decline and then increase to above normal across the domain, especially across the North-Forest subregion.

For savanna fires around the Bay subregion, weak-to-moderate emission events are associated with slightly warmer than normal conditions, with warming along the coast for moderate events. For high emissions events, the coastal warming intensifies while strong cooling develops over northern California and Nevada. Wind anomalies during weak-to-moderate Bay-Savanna fires are weakly negative or near zero across California, but for higher emissions, wind anomalies across the state become increasingly positive. For the rare extreme emissions case, a

complex pattern develops, with very strong winds over the coastal terrain north of the Bay Area and near the crest of the Sierra Nevada but reduced winds over the eastern portion of the Bay domain. Such strong winds in the western portion may explain the concentration of high emissions fire in the western Bay subregion (
Figure 3).

Considering savanna fires over southern California, including the well-known Santa Ana events, the temperature anomalies across California are very weak or even negative for the weak-to-moderate emission cases but become warmer than normal as emissions increase. For the largest emissions events, warming increases along the coastal zone and within the interior of California while Nevada becomes cooler than normal. For weak-to-moderate emissions, winds across the subregion are near normal. But as emissions over the subregion increase to higher values, the winds become much stronger over southern California, consistent with Santa Ana events.

An essential finding of this research is that there are substantial differences in the meteorological forcing associated with different levels of wildfire emissions and that such forcing has substantial spatial variations. Although there are commonalities in the meteorology associated with geographically proximate fires in savanna and forest, there are also notable differences. This thesis has also shown the differences in the seasonality of fires for differing fuels and for fires of varying emissions amounts. A key message of this thesis is that both dryness (large VPD) and strong winds are essential for the highest emissions fires, and that both should be considered when projecting future changes in wildfire frequency and severity.

Based on this research, there are several follow-up tasks that could be productive. Long-term observed trends in the VPD and wind criteria can be determined for California and its subregions. Future projections of the criteria can be determined using regional climate model

output applying realistic emissions scenarios (e.g., SSP 4.5). In addition, this thesis would be enhanced by using higher-resolution emissions, land use, and meteorological data.

.

.

BIBLIOGRAPHY

Abatzoglou, J. T., and C. A. Kolden, 2013: Relationships between climate and macroscale area burned in the western United States. *Int. J. Wildland Fire*, **22**, 1003–1020, https://doi.org/10.1071/WF13019.

——, and A. P. Williams, 2016: Impact of anthropogenic climate change on wildfire across western US forests. *PNAS*, **113**, 11770–11775, https://doi.org/10.1073/pnas.1607171113.

——, R. Barbero, and N. J. Nauslar, 2013: Diagnosing Santa Ana Winds in Southern California with Synoptic-Scale Analysis. *Weather and Forecasting*, **28**, 704–710, https://doi.org/10.1175/WAF-D-13-00002.1.

——, D. S. Battisti, A. P. Williams, W. D. Hansen, B. J. Harvey, and C. A. Kolden, 2021a: Projected increases in western US forest fire despite growing fuel constraints. *Commun Earth Environ*, **2**, 1–8, https://doi.org/10.1038/s43247-021-00299-0.

——, D. E. Rupp, L. W. O'Neill, and M. Sadegh, 2021b: Compound Extremes Drive the Western Oregon Wildfires of September 2020. *Geophysical Research Letters*, **48**, e2021GL092520, https://doi.org/10.1029/2021GL092520.

Abolafia-Rosenzweig, R., C. He, and F. Chen, 2022: Winter and spring climate explains a large portion of interannual variability and trend in western U.S. summer fire burned area. *Environ. Res. Lett.*, **17**, 054030, https://doi.org/10.1088/1748-9326/ac6886.

Addison, P., and T. Oommen, 2020: Post-fire debris flow modeling analyses: case study of the post-Thomas Fire event in California. *Nat Hazards*, **100**, 329–343, https://doi.org/10.1007/s11069-019-03814-x.

Agee, J. K., 1993: *Fire ecology of Pacific Northwest forests*. Island Press,.

——, and C. N. Skinner, 2005: Basic principles of forest fuel reduction treatments. *Forest Ecology and Management 211: 83-96*, **211**, 83–96, https://doi.org/10.1016/j.foreco.2005.01.034.

Akagi, S. K., R. J. Yokelson, C. Wiedinmyer, M. J. Alvarado, J. S. Reid, T. Karl, J. D. Crounse, and P. O. Wennberg, 2011: Emission factors for open and domestic biomass burning for use in atmospheric models. *Atmospheric Chemistry and Physics*, **11**, 4039.

Anderson, D. B., 1936: Relative Humidity or Vapor Pressure Deficit. *Ecology*, **17**, 277–282, https://doi.org/10.2307/1931468.

Andrews, P. L., M. G. Cruz, and R. C. Rothermel, 2013: Examination of the wind speed limit function in the Rothermel surface fire spread model. *International Journal of Wildland Fire. doi: http://dx.doi.org/10.1071/WF12122*, https://doi.org/10.1071/WF12122.

Associated Press, 2018: It will cost more than $3 billion to clean debris after California wildfires. *NBC News*,. https://www.nbcnews.com/news/us-news/california-wildfires-costs-soar-past-last-year-s-records-n946856 (Accessed December 2, 2020).

Balch, J. K., B. A. Bradley, J. T. Abatzoglou, R. C. Nagy, E. J. Fusco, and A. L. Mahood, 2017: Human-started wildfires expand the fire niche across the United States. *PNAS*, **114**, 2946–2951, https://doi.org/10.1073/pnas.1617394114.

Baltzer, J. L., and Coauthors, 2021: Increasing fire and the decline of fire adapted black spruce in the boreal forest. *PNAS*, **118**, https://doi.org/10.1073/pnas.2024872118.

Barrett, S. W., and S. F. Arno, 1999: Indian Fires in the Northern Rockies. *Indians, Fire and the Land in the Pacific Northwest*, Oregon State University Press.

Beck, H. E., N. E. Zimmermann, T. R. McVicar, N. Vergopolan, A. Berg, and E. F. Wood, 2018: Present and future Köppen-Geiger climate classification maps at 1-km resolution. *Sci Data*, **5**, 180214, https://doi.org/10.1038/sdata.2018.214.

Bond, W. J., and J. J. Midgley, 1995: Kill Thy Neighbour: An Individualistic Argument for the Evolution of Flammability. *Oikos*, **73**, 79–85, https://doi.org/10.2307/3545728.

——, K. J. M. Dickinson, and A. F. Mark, 2004: What Limits the Spread of Fire-Dependent Vegetation? Evidence from Geographic Variation of Serotiny in a New Zealand Shrub. *Global Ecology and Biogeography*, **13**, 115–127.

Bowden, L. W., J. R. Huning, C. F. Hutchinson, and C. W. Johnson, 1974: Satellite Photograph Presents First Comprehensive View of Local Wind: The Santa Ana. *Science*, **184**, 1077–1078.

Bowers, C. L., 2018: The Diablo Winds of Northern California: Climatology and Numerical Simulations. San Jose State University, .

Bradshaw, L. S., J. E. Deeming, R. E. Burgan, and J. D. Cohen, 1984: The 1978 National Fire-Danger Rating System: technical documentation. *General Technical Report INT-169. Ogden, UT: U.S. Department of Agriculture, Forest Service, Intermountain Forest and Range Experiment Station. 44 p.*, **169**, https://doi.org/10.2737/INT-GTR-169.

Bradstock, R. A., A. M. Gill, and R. J. Wiliams, eds., 2012: *Flammable Australia*. CSIRO,.

Brewer, M. J., and C. B. Clements, 2020: The 2018 Camp Fire: Meteorological Analysis Using In Situ Observations and Numerical Simulations. *Atmosphere*, **11**, 47, https://doi.org/10.3390/atmos11010047.

Brey, S. J., E. A. Barnes, J. R. Pierce, A. L. S. Swann, and E. V. Fischer, 2021: Past Variance and Future Projections of the Environmental Conditions Driving Western U.S. Summertime Wildfire Burn Area. *Earth's Future*, **9**, e2020EF001645, https://doi.org/10.1029/2020EF001645.

Burgan, R. E., R. W. Klaver, and J. M. Klarer, 1998: Fuel models and fire potential from satellite and surface observations. *International Journal of Wildland Fire*, **8**, 12, https://doi.org/10.1071/WF9980159.

Burke, M., A. Driscoll, S. Heft-Neal, J. Xue, J. Burney, and M. Wara, 2021: The changing risk and burden of wildfire in the United States. *PNAS*, **118**, https://doi.org/10.1073/pnas.2011048118.

Cao, Y., and R. G. Fovell, 2016: Downslope Windstorms of San Diego County. Part I: A Case Study. *Monthly Weather Review*, **144**, 529–552, https://doi.org/10.1175/MWR-D-15-0147.1.

Chandler, C. C., P. Cheney, P. Thomas, L. Trabaud, and D. Williams, 1983: *Fire in forestry*. Wiley,.

Clark, W., 1804: The Journals of Lewis and Clark, by Meriwether Lewis and And William Clark. https://www.gutenberg.org/files/8419/8419-h/8419-h.htm (Accessed May 5, 2021).

Coen, J. L., E. N. Stavros, and J. A. Fites-Kaufman, 2018: Deconstructing the King megafire. *Ecological Applications*, **28**, 1565–1580, https://doi.org/10.1002/eap.1752.

Collins, B. M., R. G. Everett, and S. L. Stephens, 2011: Impacts of fire exclusion and recent managed fire on forest structure in old growth Sierra Nevada mixed-conifer forests. *Ecosphere. 2(4): 1-14*, **2**, 1–14, https://doi.org/10.1890/ES11-00026.1.

Corby, G. A., 1954: THE AIRFLOW OVER MOUNTAINS. A review of the state of current knowledge. *Quarterly Journal of the Royal Meteorological Society*, **80**, 491–521, https://doi.org/10.1002/qj.49708034602.

Dennison, P. E., S. C. Brewer, J. D. Arnold, and M. A. Moritz, 2014: Large wildfire trends in the western United States, 1984–2011. *Geophysical Research Letters*, **41**, 2928–2933, https://doi.org/10.1002/2014GL059576.

Durran, D., 1990: Mountain Waves and Downslope Winds. *Am. Meteorol. Soc. Monogr.*, Vol. 23 of, 59–81.

Edinger, J. G., 1963: Modification of the Marine Layer over Coastal Southern California. *Journal of Applied Meteorology (1962-1982)*, **2**, 706–712.

Fernandez-Pello, A. C., 2017: Wildland fire spot ignition by sparks and firebrands. *Fire Safety Journal*, **91**, 2–10, https://doi.org/10.1016/j.firesaf.2017.04.040.

Field, D., and D. A. Jensen, 2005: Humans, Fire, and Forests: Expanding the Domain of Wildfire Research. *Society & Natural Resources*, **18**, 355–362, https://doi.org/10.1080/08941920590915251.

Finney, M. A., 1998: FARSITE: Fire Area Simulator-model development and evaluation. *Res. Pap. RMRS-RP-4, Revised 2004. Ogden, UT: U.S. Department of Agriculture, Forest Service, Rocky Mountain Research Station. 47 p.*, **4**, https://doi.org/10.2737/RMRS-RP-4.

Fosberg, M., 1978: Weather in wildland fire management: the fire weather index. Conference on Sierra Nevada Meteorology, Lake Tahoe, CA, 1–4.

Franklin, J. F., and T. A. Spies, 1991: The structure of natural young, mature, and old-growth Douglas-fir forests in Oregon and Washington. *Wildlife and vegetation of unmanaged Douglas-fir forests. Gen. Tech. Rep. PNW-285. Portland, OR: U.S. Department of Agriculture, Forest Service, Pacific Northwest Research Station*, U.S. Department of Agriculture, Forest Service, Pacific Northwest Research Station, 91–109.

——, and Coauthors, 2002: Disturbances and structural development of natural forest ecosystems with silvicultural implications, using Douglas-fir forests as an example. *Forest Ecology and Management*, **155**, 399–423, https://doi.org/10.1016/S0378-1127(01)00575-8.

——, K. N. Johnson, and D. L. Johnson, 2018: *Ecological Forest Management*. 1st ed. Waveland Press, Inc, 646 pp.

Friedl, M. A., and Coauthors, 2002: Global land cover mapping from MODIS: algorithms and early results. *Remote Sensing of Environment*, **83**, 287–302, https://doi.org/10.1016/S0034-4257(02)00078-0.

Giglio, L., J. T. Randerson, and G. R. van der Werf, 2013: Analysis of daily, monthly, and annual burned area using the fourth-generation global fire emissions database (GFED4). *Journal of Geophysical Research: Biogeosciences*, **118**, 317–328, https://doi.org/10.1002/jgrg.20042.

Halofsky, J. E., D. L. Peterson, and B. J. Harvey, 2020: Changing wildfire, changing forests: the effects of climate change on fire regimes and vegetation in the Pacific Northwest, USA. *Fire Ecology*, **16**, 1–26, https://doi.org/10.1186/s42408-019-0062-8.

Hammer, R., V. Radeloff, J. Fried, and S. Stewart, 2007: Wildland–urban interface housing growth during the 1990 in California, Oregon, and Washington. *International Journal of Wildland Fire*, **16**, 255–265, https://doi.org/10.1071/WF05077.

Heinsch, F. A., P. L. Andrews, and D. Tirmenstein, 2017: How to generate and interpret fire characteristics charts for the U.S. fire danger rating system. *Gen. Tech. Rep. RMRS-GTR-363. Fort Collins, CO: U.S. Department of Agriculture, Forest Service, Rocky Mountain Research Station. 62 p.*, **363**, https://doi.org/10.2737/RMRS-GTR-363.

Holton, J. R., 1992: *An introduction to dynamic meteorology*. 3rd ed. Academic Press, 511 pp.

Hood, S., I. Abrahamson, and C. A. Cansler, 2018: Fire resistance and regeneration characteristics of Northern Rockies tree species.

https://www.fs.fed.us/database/feis/pdfs/other/FireResistRegen.html (Accessed October 21, 2021).

Hughes, M., and A. Hall, 2010: Local and synoptic mechanisms causing Southern California's Santa Ana winds. *Clim Dyn*, **34**, 847–857, https://doi.org/10.1007/s00382-009-0650-4.

Intergovernmental Panel on Climate Change (IPCC), C. C. (2013), *The Physical Science Basis. Contribution of Working Group I to the Fifth Assessment Report of the Intergovernmental Panel on Climate Change*. Cambridge Univ. Press,.

Johnston, E. S., 1919: Evaporation compared with vapor pressure deficit and wind velocity. *Monthly Weather Review*, **47**, 30–33, https://doi.org/10.1175/1520-0493(1919)47<30:ECWVPD>2.0.CO;2.

Johnston, F. H., and Coauthors, 2012: Estimated Global Mortality Attributable to Smoke from Landscape Fires. *Environmental Health Perspectives*, **120**, 695–701.

Jones, B. A., 2017: Are we underestimating the economic costs of wildfire smoke? An investigation using the life satisfaction approach. *Journal of Forest Economics*, **27**, 80–90, https://doi.org/10.1016/j.jfe.2017.03.004.

Karter, M. J., 2008: U.S. Fire Loss for 2007. *NFPA Journal*, **102**, 46–51.

Kaur, H., 2020: The August Complex is now a "gigafire," a rare designation for a blaze that burns at least a million acres - CNN. *CNN*,. https://www.cnn.com/2020/10/06/us/gigafire-california-august-complex-trnd/index.html (Accessed May 5, 2021).

Keeley, J., H. Safford, C. Fotheringham, J. Franklin, and M. Moritz, 2009: The 2007 Southern California Wildfires: Lessons in Complexity. *Journal of Forestry*, **107**, 287–296.

——, J. Franklin, and C. D'Antonio, 2011: Fire and Invasive Plants on California Landscapes. *The Landscape Ecology of Fire*, 193–221.

Keeley, J. E., and C. J. Fotheringham, 2003: Impact of Past, Present, and Future Fire Regimes on North American Mediterranean Shrublands. *Fire and Climatic Change in Temperate Ecosystems of the Western Americas*, T.T. Veblen, W.L. Baker, G. Montenegro, and T.W. Swetnam, Eds., *Ecological Studies*, Springer, 218–262.

——, and P. H. Zedler, 2009: Large, high-intensity fire events in southern California shrublands: debunking the fine-grain age patch model. *Ecological Applications*, **19**, 69–94, https://doi.org/10.1890/08-0281.1.

——, and A. D. Syphard, 2017: Different historical fire–climate patterns in California. *International Journal of Wildland Fire*, **26**, 253268, https://doi.org/10.1071/WF16102.

——, and ——, 2018: Historical patterns of wildfire ignition sources in California ecosystems. *Int. J. Wildland Fire*, **27**, 781–799, https://doi.org/10.1071/WF18026.

——, and ——, 2019: Twenty-first century California, USA, wildfires: fuel-dominated vs. wind-dominated fires. *Fire Ecology*, **15**, 24, https://doi.org/10.1186/s42408-019-0041-0.

——, C. J. Fotheringham, and M. A. Moritz, 2004: Lessons from the October 2003. Wildfires in Southern California. *Journal of Forestry*, **102**, 26–31, https://doi.org/10.1093/jof/102.7.26.

Klimaszewski-Patterson, A., P. J. Weisberg, S. A. Mensing, and R. M. Scheller, 2018: Using Paleolandscape Modeling to Investigate the Impact of Native American–Set Fires on Pre-Columbian Forests in the Southern Sierra Nevada, California, USA. *Annals of the American Association of Geographers*, **108**, 1635–1654, https://doi.org/10.1080/24694452.2018.1470922.

Koo, E., P. J. Pagni, D. R. Weise, and J. P. Woycheese, 2010: Firebrands and spotting ignition in large-scale fires. *Int. J. Wildland Fire*, **19**, 818, https://doi.org/10.1071/WF07119.

Kramer, H. A., M. H. Mockrin, P. M. Alexandre, V. C. Radeloff, H. A. Kramer, M. H. Mockrin, P. M. Alexandre, and V. C. Radeloff, 2019: High wildfire damage in interface communities in California. *Int. J. Wildland Fire*, **28**, 641–650, https://doi.org/10.1071/WF18108.

Kucera, C. L., 1954: Some Relationships of Evaporation Rate to Vapor Pressure Deficit and Low Wind Velocity. *Ecology*, **35**, 71–75, https://doi.org/10.2307/1931406.

Lawes, M. J., A. Richards, J. Dathe, and J. J. Midgley, 2011: Bark thickness determines fire resistance of selected tree species from fire-prone tropical savanna in north Australia. *Plant Ecol*, **212**, 2057–2069, https://doi.org/10.1007/s11258-011-9954-7.

Lewis, M., 1805: The Journals of Lewis and Clark, by Meriwether Lewis and And William Clark. https://www.gutenberg.org/files/8419/8419-h/8419-h.htm#link22H_4_0114 (Accessed May 10, 2021).

Littell, J., D. McKenzie, D. Peterson, and A. Westerling, 2009: Climate and wildfire area burned in western U.S. ecoprovinces, 1916–2003. *Ecological applications : a publication of the Ecological Society of America*, **19**, 1003–1021, https://doi.org/10.1890/07-1183.1.

Liu, Y.-C., P. Di, S.-H. Chen, X. Chen, J. Fan, J. DaMassa, and J. Avise, 2020: Climatology of diablo winds in Northern California and their relationships with large-scale climate variabilities. *Clim Dyn*, https://doi.org/10.1007/s00382-020-05535-5.

Loudermilk, E. L., R. M. Scheller, P. J. Weisberg, J. Yang, T. E. Dilts, S. L. Karam, and C. Skinner, 2013: Carbon dynamics in the future forest: the importance of long-term successional legacy and climate–fire interactions. *Global Change Biology*, **19**, 3502–3515, https://doi.org/10.1111/gcb.12310.

Löw, P., 2019: The natural disasters of 2018 in figures | Munich Re Topics Online. *munichre.com*,. https://www.munichre.com/topics-online/en/climate-change-and-natural-

disasters/natural-disasters/the-natural-disasters-of-2018-in-figures.html (Accessed May 5, 2021).

Lydersen, J. M., B. M. Collins, J. D. Miller, D. L. Fry, and S. L. Stephens, 2016: Relating Fire-Caused Change in Forest Structure to Remotely Sensed Estimates of Fire Severity. *fire ecol*, **12**, 99–116, https://doi.org/10.4996/fireecology.1203099.

Marlon, J. R., and Coauthors, 2012: Long-term perspective on wildfires in the western USA. *PNAS*, **109**, E535–E543, https://doi.org/10.1073/pnas.1112839109.

Mass, C. F., and D. Ovens, 2019: The Northern California Wildfires of 8–9 October 2017: The Role of a Major Downslope Wind Event. *Bull. Amer. Meteor. Soc.*, **100**, 235–256, https://doi.org/10.1175/BAMS-D-18-0037.1.

——, and ——, 2020: The Synoptic and Mesoscale Evolution Accompanying the 2018 Camp Fire of Northern California. *Bulletin of the American Meteorological Society*, **1**, 1–45, https://doi.org/10.1175/BAMS-D-20-0124.1.

——, M. D. Albright, and D. J. Brees, 1986: The Onshore Surge of Marine Air into the Pacific Northwest: A Coastal Region of Complex Terrain. *Monthly Weather Review*, **114**, 2602–2627, https://doi.org/10.1175/1520-0493(1986)114<2602:TOSOMA>2.0.CO;2.

——, D. Ovens, R. Conrick, and J. Saltenberger, 2021: The September 2020 Wildfires over the Pacific Northwest. *Weather and Forecasting*, **36**, 1843–1865, https://doi.org/10.1175/WAF-D-21-0028.1.

Matthews, S., and S. Matthews, 2013: Dead fuel moisture research: 1991–2012. *Int. J. Wildland Fire*, **23**, 78–92, https://doi.org/10.1071/WF13005.

McClung, B., and C. F. Mass, 2020: The Strong, Dry Winds of Central and Northern California: Climatology and Synoptic Evolution. *Weather and Forecasting*, **35**, 2163–2178, https://doi.org/10.1175/WAF-D-19-0221.1.

McClure, C. D., and D. A. Jaffe, 2018: US particulate matter air quality improves except in wildfire-prone areas. *Proc Natl Acad Sci U S A*, **115**, 7901–7906, https://doi.org/10.1073/pnas.1804353115.

Mensing, S. A., J. Michaelsen, and R. Byrne, 1999: A 560-Year Record of Santa Ana Fires Reconstructed from Charcoal Deposited in the Santa Barbara Basin, California. *Quaternary Research*, **51**, 295–305, https://doi.org/10.1006/qres.1999.2035.

Minore, D., 1979: Comparative autecological characteristics of northwestern tree species;a literature review. *Gen. Tech. Rep. PNW-GTR-087. Portland, OR: U.S. Department of Agriculture, Forest Service, Pacific Northwest Research Station: 1-72*, **087**.

Moritz, M. A., T. J. Moody, M. A. Krawchuk, M. Hughes, and A. Hall, 2010: Spatial variation in extreme winds predicts large wildfire locations in chaparral ecosystems. *Geophysical Research Letters*, **37**, https://doi.org/10.1029/2009GL041735.

Morris, W. G., 1934: Forest Fires in Western Oregon and Western Washington. *Oregon Historical Quarterly*, **35**, 313–339.

Mouillot, F., and C. B. Field, 2005: Fire history and the global carbon budget: a 1°× 1° fire history reconstruction for the 20th century. *Global Change Biology*, **11**, 398–420, https://doi.org/10.1111/j.1365-2486.2005.00920.x.

Mu, M., and Coauthors, 2011: Daily and 3-hourly variability in global fire emissions and consequences for atmospheric model predictions of carbon monoxide. *Journal of Geophysical Research: Atmospheres*, **116**, https://doi.org/10.1029/2011JD016245.

Muir, P. S., and J. E. Lotan, 1985: Disturbance History and Serotiny of Pinus contorta in Western Montana. *Ecology*, **66**, 1658–1668, https://doi.org/10.2307/1938028.

Murdoch, G. P., and C. M. Gitro, 2010: Assessing critical fire weather conditions using a red flag threat index. 35th Annual Nat. Weath. Assoc. Meeting, Tucson, AZ.

Nauslar, N. J., J. T. Abatzoglou, and P. T. Marsh, 2018: The 2017 North Bay and Southern California Fires: A Case Study. *Fire*, **1**, 18, https://doi.org/10.3390/fire1010018.

O'Brien, J. J., J. K. Hiers, J. M. Varner, C. M. Hoffman, M. B. Dickinson, S. T. Michaletz, E. L. Loudermilk, and B. W. Butler, 2018: Advances in Mechanistic Approaches to Quantifying Biophysical Fire Effects. *Current Forestry Reports*, **4**, 161–177, https://doi.org/10.1007/s40725-018-0082-7.

Pagni, P. J., 1993: Causes of the 20 October 1991 Oakland Hills conflagration. *Fire Safety Journal*, **21**, 331–339, https://doi.org/10.1016/0379-7112(93)90020-Q.

Paine, R. T., M. J. Tegner, and E. A. Johnson, 1998: Compounded Perturbations Yield Ecological Surprises. *Ecosystems*, **1**, 535–545.

Parker, G., M. Davis, and S. Chapotin, 2002: Canopy light transmittance in Douglas-fir-western hemlock stands. *Tree physiology*, **22**, 147–157, https://doi.org/10.1093/treephys/22.2-3.147.

Parker, G., and Coauthors, 2004: Three-dimensional Structure of an Old-growth Pseudotsuga-Tsuga Canopy and Its Implications for Radiation Balance, Microclimate, and Gas Exchange. *Ecosystems*, https://doi.org/10.1007/s10021-004-0136-5.

Parks, S. A., and J. T. Abatzoglou, 2020: Warmer and Drier Fire Seasons Contribute to Increases in Area Burned at High Severity in Western US Forests From 1985 to 2017. *Geophysical Research Letters*, **47**, e2020GL089858, https://doi.org/10.1029/2020GL089858.

Pyne, S., and T. R. Vale, 2003: Fire, Native Peoples, and the Natural Landscape. *Restoration Ecology*, **11**, 257–259, https://doi.org/10.1046/j.1526-100X.2003.01122.x.

Pyne, S. J., 1996: *Introduction to wildland fire*. 2nd ed. Wiley,.

——, 2001: *Year of the Fires: The Story of the Great Fires of 1910*. Viking,.

Radeloff, V. C., and Coauthors, 2018: Rapid growth of the US wildland-urban interface raises wildfire risk. *PNAS*, **115**, 3314–3319, https://doi.org/10.1073/pnas.1718850115.

Rammer, W., K. H. Braziunas, W. D. Hansen, Z. Ratajczak, A. L. Westerling, M. G. Turner, and R. Seidl, 2021: Widespread regeneration failure in forests of Greater Yellowstone under scenarios of future climate and fire. *Global Change Biology*, **27**, 4339–4351, https://doi.org/10.1111/gcb.15726.

Randerson, J. T., Y. Chen, G. R. van der Werf, B. M. Rogers, and D. C. Morton, 2012: Global burned area and biomass burning emissions from small fires. *Journal of Geophysical Research: Biogeosciences*, **117**, https://doi.org/10.1029/2012JG002128.

——, and Coauthors, 2018: Development of the Global Fire Emissions Database (GFED): Toward reconciliation of top-down and bottom-up constraints on fire contributions to variability and trends in carbonaceous aerosol. *AGU Fall Meeting Abstracts*, **41**.

Rolinski, T., S. Capps, R. Fovell, Y. Cao, B. D'Agostino, and S. Vanderburg, 2016: The Santa Ana Wildfire Threat Index: Methodology and Operational Implementation. *Weather and Forecasting*, **31**, https://doi.org/10.1175/WAF-D-15-0141.1.

——, S. B. Capps, and W. Zhuang, 2019: Santa Ana Winds: A Descriptive Climatology. *Weather and Forecasting*, **34**, 257–275, https://doi.org/10.1175/WAF-D-18-0160.1.

Romme, W., M. Boyce, R. Gresswell, E. Merrill, G. Minshall, C. Whitlock, and M. Turner, 2011: Twenty Years After the 1988 Yellowstone Fires: Lessons About Disturbance and Ecosystems. *Ecosystems*, **14**, https://doi.org/10.1007/s10021-011-9470-6.

Romme, W. H., 1982: Fire and Landscape Diversity in Subalpine Forests of Yellowstone National Park. *Ecological Monographs*, **52**, 199–221, https://doi.org/10.2307/1942611.

Rossi, D., and O.-P. Kuusela, 2019: Cost Plus Net Value Change (C+NVC) Revisited: A Sequential Formulation of the Wildfire Economics Model. *Forest Science*, **65**, 125–136, https://doi.org/10.1093/forsci/fxy046.

Rothermel, R. C., 1972: A mathematical model for predicting fire spread in wildland fuels. *Res. Pap. INT-115. Ogden, UT: U.S. Department of Agriculture, Intermountain Forest and Range Experiment Station. 40 p.*, **115**.

Routley, J. G., 1992: *The East Bay hills fire, Oakland-Berkeley, California (October 19-22, 1991)*. Federal Emergency Management Agency, USFire Administration, National Fire Data Center,.

Schoennagel, T., T. T. Veblen, and W. H. Romme, 2004: The Interaction of Fire, Fuels, and Climate across Rocky Mountain Forests. *BioScience*, **54**, 661–676, https://doi.org/10.1641/0006-3568(2004)054[0661:TIOFFA]2.0.CO;2.

Schroeder, M. J., and Coauthors, 1964: Synoptic weather types associated with critical fire weather. *Berkeley, CA: USDA Forest Service, Pacific Southwest Forest and Range Experiment Station. 503 p*,.

Schwartz, M. W., and A. D. Syphard, 2021: Fitting the solutions to the problems in managing extreme wildfire in California. *Environ. Res. Commun.*, **3**, 081005, https://doi.org/10.1088/2515-7620/ac15e1.

Scott, A. C., 2000: The Pre-Quaternary history of fire. *Palaeogeography, Palaeoclimatology, Palaeoecology*, **164**, 281–329, https://doi.org/10.1016/S0031-0182(00)00192-9.

Scott, A. C., D. M. J. S. Bowman, W. J. Bond, S. J. Pyne, and M. E. Alexander, 2014: *Fire on Earth: An Introduction*. John Wiley & Sons, Incorporated,.

Scott, J. H., and R. E. Burgan, 2005: Standard fire behavior fuel models: a comprehensive set for use with Rothermel's surface fire spread model. *Gen. Tech. Rep. RMRS-GTR-153. Fort Collins, CO: U.S. Department of Agriculture, Forest Service, Rocky Mountain Research Station. 72 p.*, **153**, https://doi.org/10.2737/RMRS-GTR-153.

Seager, R., A. Hooks, A. P. Williams, B. Cook, J. Nakamura, and N. Henderson, 2015: Climatology, Variability, and Trends in the U.S. Vapor Pressure Deficit, an Important Fire-Related Meteorological Quantity*. https://doi.org/10.1175/JAMC-D-14-0321.1.

Sharples, J. J., R. H. D. McRae, R. O. Weber, and A. M. Gill, 2009a: A simple index for assessing fire danger rating. *Environmental Modelling & Software*, **24**, 764–774, https://doi.org/10.1016/j.envsoft.2008.11.004.

——, ——, ——, and ——, 2009b: A simple index for assessing fuel moisture content. *Environmental Modelling & Software*, **24**, 637–646, https://doi.org/10.1016/j.envsoft.2008.10.012.

Shi, H., and Coauthors, 2019: Modeling Study of the Air Quality Impact of Record-Breaking Southern California Wildfires in December 2017. *Journal of Geophysical Research: Atmospheres*, **124**, 6554–6570, https://doi.org/10.1029/2019JD030472.

Simard, M., W. H. Romme, J. M. Griffin, and M. G. Turner, 2011: Do mountain pine beetle outbreaks change the probability of active crown fire in lodgepole pine forests? *Ecological Monographs*, **81**, 3–24.

Skinner, C. N., and C. Chang, 1996: Fire regimes, past and present. *In: Sierra Nevada Ecosystem Project: Final report to Congress. Vol. II. Assessments and Scientific Basis for Management Options. Wildland Resources Center Report No. 37. Centers for Water and Wildland Resources, University of California, Davis. 1041-1069*, **2**, 1041–1069.

Smith, C., B. J. Hatchett, and M. Kaplan, 2018: A Surface Observation Based Climatology of Diablo-Like Winds in California's Wine Country and Western Sierra Nevada. *Fire*, **1**, 25, https://doi.org/10.3390/fire1020025.

Sommers, W., S. Coloff, and S. Conard, 2011: Synthesis of Knowledge: Fire History and Climate Change. *JFSP Synthesis Reports*,.

Spies, T. A., and S. P. Cline, 1988: Coarse woody debris in forests and plantations of coastal Oregon. *From the forest to the sea: a story of fallen trees. Gen. Tech. Rep. PNW-GTR-229*, U.S. Department of Agriculture, Forest Service, Pacific Northwest Research Station; U.S. Department of the Interior, Bureau of Land Management, 5–24.

Srock, A. F., J. J. Charney, B. E. Potter, and S. L. Goodrick, 2018: The Hot-Dry-Windy Index: A New Fire Weather Index. *Atmosphere*, **9**, 279, https://doi.org/10.3390/atmos9070279.

Steel, Z. L., H. D. Safford, and J. H. Viers, 2015: The fire frequency-severity relationship and the legacy of fire suppression in California forests. *Ecosphere*, **6**, art8, https://doi.org/10.1890/ES14-00224.1.

Stephens, E., 1968: The marine layer and its relation to a smog episode in Riverside, California. *Atmospheric Environment (1967)*, **2**, 393–396, https://doi.org/10.1016/0004-6981(68)90008-5.

Stephens, S., and B. Collins, 2004: Fire Regimes of Mixed Conifer Forests in the North-Central Sierra Nevada at Multiple Spatial Scales. *Northwest Science*, **78**.

Swanson, M., J. Franklin, R. Beschta, C. Crisafulli, D. Dellasala, R. Hutto, D. Lindenmayer, and F. Swanson, 2010: The forgotten stage of forest succession: Early-successional ecosystems on forest sites. *Frontiers in Ecology and The Environment - FRONT ECOL ENVIRON*, **9**, https://doi.org/10.1890/090157.

Swanson, M. E., N. M. Studevant, J. L. Campbell, and D. C. Donato, 2014: Biological associates of early-seral pre-forest in the Pacific Northwest. *Forest Ecology and Management*, **324**, 160–171, https://doi.org/10.1016/j.foreco.2014.03.046.

Swetnam, T., and C. Baisan, 1996: Historical Fire Regime Patterns in the Southwestern United States Since AD 1700. *Fire Effects in Southwestern Fortest : Proceedings of the 2nd La Mesa Fire Symposium*, 11–32.

Syphard, A. D., and J. E. Keeley, 2015: Location, timing and extent of wildfire vary by cause of ignition. *Int. J. Wildland Fire*, **24**, 37–47, https://doi.org/10.1071/WF14024.

——, H. Rustigian-Romsos, M. Mann, E. Conlisk, M. A. Moritz, and D. Ackerly, 2019: The relative influence of climate and housing development on current and projected future fire patterns and structure loss across three California landscapes. *Global Environmental Change*, **56**, 41–55, https://doi.org/10.1016/j.gloenvcha.2019.03.007.

Taylor, A. H., and M. N. Solem, 2001: Fire Regimes and Stand Dynamics in an Upper Montane Forest Landscape in the Southern Cascades, Caribou Wilderness, California. *The Journal of the Torrey Botanical Society*, **128**, 350–361, https://doi.org/10.2307/3088667.

Telford, T., 2019: PG&E, the nation's biggest utility company, files for bankruptcy after California wildfires. *The Washington Post*,.

Turner, M. G., W. W. Hargrove, R. H. Gardner, and W. H. Romme, 1994: Effects of Fire on Landscape Heterogeneity in Yellowstone National Park, Wyoming. *Journal of Vegetation Science*, **5**, 731–742, https://doi.org/10.2307/3235886.

Van de Water, K. M., and H. D. Safford, 2011: A Summary of Fire Frequency Estimates for California Vegetation before Euro-American Settlement. *fire ecol*, **7**, 26–58, https://doi.org/10.4996/fireecology.0703026.

Van Wagner, C. E., 1974: Structure of the Canadian Forest Fire Weather Index. **1333**.

Wang, S. S.-C., Y. Qian, L. R. Leung, and Y. Zhang, 2021: Identifying Key Drivers of Wildfires in the Contiguous US Using Machine Learning and Game Theory Interpretation. *Earth's Future*, **9**, e2020EF001910, https://doi.org/10.1029/2020EF001910.

van der Werf, G. R., and Coauthors, 2017: Global fire emissions estimates during 1997–2016. *Earth System Science Data*, **9**, 697–720, https://doi.org/10.5194/essd-9-697-2017.

Werth, P. A., and Coauthors, 2016: Synthesis of knowledge of extreme fire behavior: volume 2 for fire behavior specialists, researchers, and meteorologists. *Gen. Tech. Rep. PNW-GTR-891. Portland, OR: U.S. Department of Agriculture, Forest Service, Pacific Northwest Research Station. 258 p.*, **891**, https://doi.org/10.2737/PNW-GTR-891.

Westerling, A. L., D. R. Cayan, T. J. Brown, B. L. Hall, and L. G. Riddle, 2004: Climate, Santa Ana Winds and autumn wildfires in southern California. *Eos, Transactions American Geophysical Union*, **85**, 289–296, https://doi.org/10.1029/2004EO310001.

Williams, A. P., J. T. Abatzoglou, A. Gershunov, J. Guzman-Morales, D. A. Bishop, J. K. Balch, and D. P. Lettenmaier, 2019: Observed Impacts of Anthropogenic Climate Change on Wildfire in California. *Earth's Future*, **7**, 892–910, https://doi.org/10.1029/2019EF001210.

Xie, Y., M. Lin, and L. W. Horowitz, 2020: Summer PM2.5 Pollution Extremes Caused by Wildfires Over the Western United States During 2017–2018. *Geophysical Research Letters*, **47**, e2020GL089429, https://doi.org/10.1029/2020GL089429.